

ROSAT BLANK FIELD SOURCES I: SAMPLE SELECTION AND ARCHIVAL DATA

I. CAGNONI^{1,2,3}, M. ELVIS³, D.W. KIM³, F. NICASTRO³
 AND

A. CELOTTI²

¹ Dipartimento di Scienze, Università dell'Insubria, Como, Italy

² SISSA, Via Beirut 4 -34138, Trieste, Italy

³ Harvard-Smithsonian Center for Astrophysics, 60 Garden Street, Cambridge, MA 02138, USA

1

Accepted version. To appear in ApJ main journal

ABSTRACT

We have identified a population of ‘blank field sources’ (or ‘blanks’) among the *ROSAT* bright unidentified X-ray sources with faint optical counterparts. The extreme X-ray over optical flux ratio of blanks is not compatible with the main classes of X-ray emitters except for extreme BL Lacertae objects.

From the analysis of *ROSAT* archival data we found no indication of variability and evidence for only three sources, out of 16, needing absorption in excess of the Galactic value. We also found evidence for an extended nature for only one of the 5 blanks with a serendipitous HRI detection; this source (1WGA J1226.9+3332) was confirmed as a $z=0.89$ cluster of galaxies. Palomar images reveal the presence of a red ($O-E \geq 2$) counterpart in the X-ray error circle for 6 blanks. The identification process brought to the discovery of another high z cluster of galaxies, one (possibly extreme) BL Lac, two ultraluminous X-ray sources in nearby galaxies and two apparently normal type 1 AGNs. These AGNs, together with 4 more AGN-like objects seem to form a well defined group: they present unabsorbed X-ray spectra but red Palomar counterparts. We discuss the possible explanations for the discrepancy between the X-ray and optical data, among which: a suppressed big blue bump emission, an extreme dust to gas ($\sim 40-60$ the Galactic ratio), a high redshift ($z \geq 3.5$) QSO nature, an atypical dust grain size distribution and a dusty warm absorber. These AGN-like blanks seem to be the bright (and easier to study) analogs of the sources which are found in deep *Chandra* observations. Three more blanks have a still unknown nature.

Subject headings: galaxies:nuclei – galaxies:active – galaxies: Seyfert – BL Lacertae objects: general – X-rays: galaxies – X-rays: galaxies: clusters

1. INTRODUCTION

The X-ray sky is not as well known as sometimes thought. There might exist classes of quite common sources, comprising from one to a few percent of the high Galactic latitude population, which are currently thought to be “rare” because of the difficulty of finding them. We are actively searching for such ‘minority’ populations (Kim & Elvis 1999). We have found an interesting high fraction of extreme X-ray loud sources ($\sim 7-8\%$) among the *ROSAT* high Galactic latitude sources at all fluxes: (this paper, Bade et al. 1995; Schmidt et al. 1998). Here we designate as ‘blank field sources’ or ‘blanks’ all the bright *ROSAT* PSPC (Position Sensitive Proportional Counter) X-ray sources ($f_X > 10^{-13}$ erg cm⁻² s⁻¹) with no optical counterpart on the Palomar Observatory Sky Survey (POSS) (to $O=21.5^2$) within their $39''$ (99%) radius error circle. For comparison, at these X-ray fluxes a normal type 1 AGN should appear on the POSS some 3.5 magnitudes brighter ($O \sim 18$). The nature of these sources has never been systematically investigated before, and their nature is still mysterious. We decided to select these sources and to study them to understand their nature because of the important cosmological and astrophysical consequences that could derive from their identification.

The outline of this paper is the following: we introduce *ROSAT* blank field sources, review the open possibilities for their nature and the important consequences that could derive from the

identification of these sources in § 2; we present the selection criteria used for the definition of the sample in § 3, while § 4, 6 and 7 focus on the analysis of *ROSAT*, *ASCA* and radio archival data. § 7 contains detailed information on the sources and the discussion, while in § 8 we compare the results of this work with the findings of other surveys. A summary is presented in § 9. We will use $H_0=75$ km s⁻¹ Mpc⁻¹ and $q_0=0.5$; errors represent 1σ confidence levels, unless explicitly stated otherwise.

2. POTENTIAL CLASSES OF BLANK FIELD SOURCES

Blank field sources are extreme X-ray loud objects with $f_X/f_V > 10^3$. The Maccacaro et al. (1988) nomograph allows us to compare this f_X/f_V with that typical of other classes of objects. Normal quasars and AGN have $0.1 < f_X/f_V < 10$; normal galaxies have only $10^{-2} < f_X/f_V < 10^{-1}$; while a high luminosity cluster of galaxies ($L_X = 10^{45}$ erg s⁻¹) would have a first ranked elliptical with $L_{gal} = 10L^*(= 10^{11.5}L_\odot)$ giving $f_X/f_V \sim 8$. The only known class of X-ray emitting objects that can reach such extreme f_X/f_V are BL Lacertae objects, which can have f_X/f_V up to ~ 35 (Maccacaro et al. 1988).

There are however several types of hypothesized objects that would appear as blank field sources. We briefly describe these below.

2.1. Extreme BL Lacertae objects

¹email: Ilaria Cagnoni: ilaria.cagnoni@uninsubria.it

²O-band effective wavelength = 4100 Å; passband = 1100 Å

³We follow the f_X/f_V definition of Maccacaro et al. (1988)

“Normal” BL Lacs are expected for $f_X/f_V < 35$ (e.g. Macacaro et al. 1988), but given the range of f_X/f_V spanned by blanks more extreme BL Lacs, with the SED peaking at energies higher than the *ROSAT* band are needed. This peak could be either the low energy (synchrotron) or the high energy (inverse Compton) one shifted appropriately. Fossati et al (1998) show that these two peaks do shift systematically with luminosity. In the first case, these indeed would be faint BL Lacs, with the synchrotron peak at $1 < E \leq 10$ keV; some such extreme BL Lacs have been found recently by e.g. Costamante et al. (2001). No examples of blazars with an inverse Compton peak lying in the 1-10 keV range are known so far, but the study of *ROSAT* blank field sources could potentially discover them.

2.2. Isolated Neutron Stars (INS) or Isolated Black Holes (IBH)

Blank field sources could be identified with old isolated neutron stars (INS) or isolated black holes (IBH), which could be observable due to accretion from the interstellar medium (“accretors”). INS can also be visible in the soft X-ray band when they are young and hot (“coolers”) due to thermal emission of their hot surface (e.g. Treves et al. 2000; Popov et al. 2002). Old INS are expected to have $f_X/f_V > 100-1000$ (Maoz, Ofek & Shemi, 1997). and extremely soft X-ray spectra and emission in the UV. The active search for INS has produced 7 strong candidates (Stoeckel et al. 1995; Walter, Wolk & Neuhauser 1996; Haberl et al. 1997; Haberl, Motch & Pietsch 1998; Schwöpe et al. 1999; Motch et al. 1999, Haberl, Pietsch & Motch 1999; Zampieri et al. 2001), but their very nature is not yet clear. The large initial velocity found for one of these sources (~ 200 km s $^{-1}$ found by Walter (2001) for RX J1856-3754) supports the “cooler” origin, while no proof of the existence of “accreting” old INS has been found. Being nearby INS and IBH (~ 100 pc) will be quasi-isotropically distributed on the sky. The predicted number counts for old INS are highly uncertain, ranging from $\sim 1/\text{deg}^2$ (Madau & Blaes 1994) to much smaller values (e.g. Colpi et al. 1998). At the predicted number of old INSs strongly depends on the properties of their progenitors (young neutron stars in the pulsar phase), such as the velocity distribution and the magnetic field decay, the spatial density, or an upper limit on it, can be used to constrain neutron stars physics (e.g. Colpi et al. 1998; Livio, Xu & Frank, 1998; Popov et al. 2000).

2.3. Peculiar AGNs

Normal type 1 AGNs with $f_X > 10^{-13}$ erg cm $^{-2}$ s $^{-1}$ have $O \sim 18$. Obscured AGNs could appear as blanks if their O-band absorption is $A_O > 3.5$ mag, which corresponds to a local $N_H > 4 \times 10^{21}$ cm $^{-2}$. Possibilities for absorbed AGNs with $f_X > 10^{-13}$ erg cm $^{-2}$ s $^{-1}$ in the *ROSAT* PSPC are:

2.3.1. Quasar-2s

QSO-2s would be high luminosity, high redshift, heavily obscured quasars, the bright analogs of the well known Seyfert 2s at $z \gg 0.5$. QSO-2s and Low Mass Seyfert-2 (LMSy2) galaxies are the “missing links” of the unifying models of AGN (Urry & Padovani 1995) and their existence is still debated (e.g. Halpern, Turner & George 1999). A large number of QSO-2s is also postulated by the models of synthesis of the X-ray background above 2 keV to reproduce the observed number counts at bright fluxes (Comastri et al. 2001, Gilli, Salvati & Hasinger 2001). Thus a knowledge of their number density is fundamental to our understanding of the X-ray sky and should be the site

where a large fraction of the energy of the universe is generated (Fabian & Iwasawa 1999; Elvis, Risaliti & Zamorani, 2002).

In spectral terms we would expect: (a) strong optical reddening; (b) soft X-ray absorption; (c) recovery of the X-ray intrinsic emission in the PSPC energy range. QSO-2s should then have flat PSPC spectra and an observed f_X/f_V enhanced by the redshift K-correction. For moderate absorbing columns ($N_H \sim 10^{22} - 10^{23}$ cm $^{-2}$) QSO-2s would be visible in the PSPC because their redshift has the effect of lowering the observed absorption; for higher column densities the direct emission could be completely absorbed, but a scattered component could still allow the source detection.

In order to quantify the expected X-ray properties, we simulated these two QSO-2 scenarios assuming, for the moderately absorbed case, a rest frame absorbed ($N_H = 5 \times 10^{22}$ cm $^{-2}$) power law model ($\Gamma = 1.7$) at $z=1.0$ with an unabsorbed $L_{(0.5-2.4\text{keV})} = 1.8 \times 10^{45}$ erg s $^{-1}$. We also included a neutral iron line at $E_{Fe} = 6.4$ keV and equivalent width of 0.15 keV. The simulated QSO-2 is detected by the *ROSAT* PSPC with a count rate (CR) of ~ 0.01 counts s $^{-1}$ corresponding to a WGACAT (0.05-2.5 keV) flux of 2.8×10^{-13} erg cm $^{-2}$ s $^{-1}$.

For the highly absorbed case we model the spectrum as the sum of an absorbed spectrum and a scattered component.

$$f(E) = e^{-\sigma N_H E^{-\Gamma}} + K E^{-\Gamma} \text{ at } z=1.0$$

where σ is the neutral H cross section for absorption, $N_H \geq 10^{24}$ cm $^{-2}$ in the rest frame, $\Gamma = 1.7$ and $K = 0.1$ indicates a 10% scattered component. With the assumed values of N_H the direct component is completely blocked by the absorbing material. A QSO with an unabsorbed luminosity of $L_{(0.5-2.4\text{keV})} \geq 10^{46}$ erg s $^{-1}$ would be detected as scattered light in the *ROSAT* PSPC band with a WGACAT flux of $\geq 10^{-13}$ erg cm $^{-2}$ s $^{-1}$.

Both would thus be included among blank field sources.

2.3.2. Low Mass Seyfert 2

LMSy 2 are Seyfert 2 galaxies powered by a relatively low mass obscured black hole ($M_{bh} \sim 10^7 M_\odot$). These would be the obscured analogs of the Narrow Line Seyfert 1s. Their low mass would shift the peak of the big blue bump (BBB) disk emission ($T_{peak} \sim M_{bh}^{1/4}$) around 100 eV. As a result their spectra would be enhanced in the soft X-ray band and suppressed in the optical. RE 1034+396 (Puchnarewicz et al. 1995; 2001) shows that this does indeed occur in NLSy 1. We simulated the LMSy2 case assuming an absorption of 5×10^{22} cm $^{-2}$, a thermal component of $kT = 150$ eV, a power law with $\Gamma = 2.2$. We normalized the model to have a ratio between the thermal and power law component matching what observed in Narrow Line Sy 1s (Nicastro, Fiore & Matt, 1999) and to have an unabsorbed luminosity at $z=0.002$ of $L_{(0.5-2.4\text{keV})} = 4 \times 10^{42}$ erg s $^{-1}$. The simulated LMSy2 is detected in the *ROSAT* PSPC with a count rate of 0.015 counts s $^{-1}$ corresponding to a 0.5-2.4 keV flux of 2.4×10^{-13} erg cm $^{-2}$ s $^{-1}$. Thus obscuration, even by large amounts of molecular matter and cold gas ($N_H = 10^{22} - 10^{23}$ cm $^{-2}$), would still allow the detection of the soft X-ray source emission because it is so intrinsically strong, but would harden the observed X-ray spectra.

2.3.3. AGNs with no big blue bump

Virtually all type 1 AGNs have optical-ultraviolet spectra dominated by the BBB component from the accretion disk (Malkan & Sargent, 1982; Elvis & Lawrence, 1982; Elvis et al. 1994) There are however radiatively inefficient mechanisms for

accretion. An example of this are ‘advection dominated accretion flows’ (ADAFs) (e.g. Narayan & Yi, 1994), where most of the energy is stored in the gas and advected toward the hole and only a small fraction is radiated. The result is a suppression of the optical-UV-EUV BBB emission (see Figure 1 of Narayan et al. (1998) for a comparison of ADAF emission to the standard Shakura-Sunyaev (1973) thin disk emission).

Radiatively inefficient accretion has been proposed to account for the spectra of Galactic black holes X-ray binaries (BHXBs) and Sagittarius A* (Narayan et al. 1998). Finding radiatively inefficient accretion among blanks could shade light on the physics and history of the accretion process in AGN and possibly strengthen the AGN-BHXB connection.

2.4. Unusual clusters of galaxies

2.4.1. High Redshift Clusters of Galaxies

At high redshifts, $z \geq 0.4$, the 4000 Å break in the spectrum of normal galaxies is shifted to wavelengths longer than the POSS O band. Any high z cluster of galaxies will then be fainter than $O=21.5$, and have $f_X/f_V > 10$. Using ‘blanks’ to locate high z clusters efficiently is a promising path to pursue. With a WGACAT (0.05-2.5 keV) $f_X > 10^{-13}$ erg cm $^{-2}$ s $^{-1}$ and assuming Galactic absorption, all such clusters will have intrinsic $L_X \geq 10^{44}$ erg s $^{-1}$. The space density of such high luminosity, and by implication massive, high z clusters of galaxies is a crucially important tool in cosmology. Their distribution and evolution is fully determined by the spectrum of primordial perturbations and cosmological parameters Ω_0 and Λ (e.g. Press & Schechter 1974). In particular, models of low Ω universe (with or without cosmological constant) predict a higher density of massive clusters at high redshifts than the high Ω models (e.g. Henry 2000, Borgani & Guzzo 2001).

Only few bright high redshift clusters have been found so far (e.g. in the EMSS, Gioia & Luppino 1994; in the RDCS Rosati et al. 1999, Della Ceca et al. 2000; in the WARPS Ebeling et al. 2000) and only 11 of them at $z > 0.5$ have a measure of their temperature (e.g. Della Ceca et al. 2000, Cagnoni et al. 2001a, Stanford et al. 2001).

Since the statistics is scanty, even a few high redshift clusters can help determining the evolution of the clusters X-ray luminosity function (e.g. Rosati et al., 1998) and any search for evolution in the luminosity-temperature ($L_X - T$) relation, related to the physical mechanisms of cooling and heating in the central cluster region (e.g. Tozzi & Norman, 2001). Since the statistics is very scanty, adding one more high z high L cluster would greatly improve such studies.

2.4.2. Dark clusters

Dark clusters are unusual clusters of galaxies with extreme high mass to light ratio. They have been searched for as “missing lens” in gravitational lenses searches (e.g. Hattori et al 1997) and one of such objects was found in the lensed system MG2016+112. The lensing mass did not show up in deep optical/IR imaging, while follow-up X-ray observations detected a $z = 1$ cluster (Hattori et al. 1997). Although *Chandra* and deeper optical searches found that the properties of the cluster AXJ2019+1127 are not so extreme as previously thought (Chartas et al. 2001), if dark clusters exist, they could be found among blanks.

2.4.3. Failed Clusters

A failed cluster would be a large overdensity of matter in the form of diffuse gas only. Galaxies have to form from clouds of gas with cooling time shorter than the Hubble time. This implies a protogalactic mass $< 10^{12} M_\odot$ (e.g. White & Frenk 1991 and references therein); in principle more massive clouds, with a longer cooling might have never collapsed to form stars in appreciable number. The result would be a large cloud of gas with no visible galaxies.

Their possible existence and number-density is connected to the efficiency of galaxy formation, which potentially constrains a number of issues such as: the spectrum of the fluctuations that gave rise to galaxies, the baryonic or non-baryonic nature of dark-matter, the value of Ω and the relative distribution of dark and baryonic matter (Tucker, Tananbaum & Remillard 1995).

The discovery of even only one failed cluster among our blanks would pose serious difficulties for the hierarchical clustering formation, which does not predict their existence.

2.5. Ultraluminous X-ray sources and binary systems in nearby galaxies

Ultraluminous X-ray sources (ULX) are objects observed in nearby galaxies, usually off the galactic center, with luminosity exceeding the Eddington limit for isotropic emission of a $1.4 M_\odot$ star (i.e. $L > 2 \times 10^{38}$ up to $\sim 10^{40}$, e.g. Fabbiano 1988; Makishima et al. 2000; Zezas et al. 2002; Colbert & Ptak 2002 and references therein). The ULX nature is still not understood and the most plausible explanations are: sub-Eddington binaries involving massive black holes ($\sim 100 M_\odot$) or binary systems with emission collimated toward our line of site (King et al. 2001) or relativistically beamed systems (microquasars). These models imply a high f_X/f_V because the optical emission is related to the companion star.

Also X-ray binaries and cataclysmic variables are known to display high X-ray over optical flux ratios and could be candidate blanks if present in an uncrowded optical region of a nearby galaxy.

2.6. Extreme variables

2.6.1. X-ray Bursts

X-ray bursts are short lived X-ray flares, which may be afterglows of Gamma Ray Bursts (GRBs). Popular GRBs scenarios such as binary coalescence of compact stars (e.g. Janka & Ruffert, 1996) or collapsars (e.g. Hartmann & MacFadyen, 1999) predict collimated flows, which should lead to collimated bursts and afterglow emission. If afterglows turn out to be less beamed than GRBs, then we expect to find a higher rate of afterglows than GRBs depending on the beaming angles. This possibility can be tested with a search for afterglows fortuitously detected during *ROSAT* PSPC pointings (e.g. Greiner et al. 2000 for a systematic search in the *ROSAT* All-Sky Survey, RASS). The *ROSAT* lightcurves of afterglows could also constrain the X-ray flux decaying rate, which can be compared with the power law slope of $\sim 1.0 - 1.5$ seen for the brighter *Beppo-SAX* afterglows (Frontera et al. 2000).

2.6.2. X-ray flares from normal galaxies

Another class of variable sources are normal galaxies which exhibit X-ray flares, probably related to the tidal disruption of a star near the central black hole (e.g. Bade, K., D., 1996). In the X-ray high-state, these galaxies exceed their quiescent f_X/f_V by up to several orders of magnitude. Timescales for the duration of the X-ray high-state are not yet well constrained; they may range from months to years.

2.6.3. Strongly variable sources

Blanks candidates also include variable sources, such as blazars or cataclysmic variables, which were caught in outburst during the *ROSAT* observations, but were quiescent in the POSS epoch, some 40 years earlier.

2.7. Summary

Quite possibly the class of blank field sources contains examples of several, or all, of these objects. The possibility of identifying blanks with sources listed above makes the study of this minority population a subject of primary importance in cosmology and astrophysics. As we will show, it is possible to make significant progress and distinguish among many of these options even without new observations, using only archival data.

3. SAMPLE SELECTION

To define our sample of ‘blank field sources’ we searched the *ROSAT* PSPC ‘WGACAT95’ (or simply ‘WGACAT’, White Giommi & Angelini 1995), a catalog containing a total of $\sim 62,000$ sources generated from *ROSAT* PSPC pointed observations using a sliding cell detect algorithm. We used the following selection criteria:

1. bright X-ray sources, with $f_X > 10^{-13}$ erg cm $^{-2}$ s $^{-1}$;
2. well detected, with a signal to noise ratio greater than 10 and a quality flag⁴ greater than 5;
3. high Galactic latitude ($|b| > 20^\circ$);
4. not within $2'$ of the target position (at which point the source density reaches the background level) to select only random, serendipitous sources;
5. location in the ‘inner circle’ of the PSPC ($r < 18'$) to have smaller positional error circles;
6. north of $\delta = -18^\circ$ in order to have measurements in the Automated Plate-measuring Machine (APM) catalog of the POSS (McMahon & Irwin 1992);
7. unidentified, with WGACAT class= 9999 and no SIMBAD or NASA Extragalactic Database identification.

The first six criteria selected 1624 sources ($\sim 3\%$ of the total). Since these sources were selected purely on their X-ray properties, they form a well defined sample from which to study the incidence of minority X-ray populations. Adding the requirement that a source has to be unidentified left 940 objects. We then searched the APM catalog for sources without any optical counterpart in the O filter (to $O=21.5$) in a radius of $26''$, which corresponds to about 95% confidence for X-ray sources within $18'$ of the PSPC detector center (Boyle et al. 1995).

We note that with a B band (similar to the Palomar O-band) source density of 1000-2000 sources deg $^{-2}$ at $B \sim 21.5-22$ (e.g. Prandoni et al. 1999; Huang et al. 2001) there is a $\sim 15-35\%$ probability for each PSPC $26''$ error circle⁵ of containing a source by chance. This implies that many other PSPC sources

might be ‘blanks’ if we had a smaller uncertainty on the X-ray positions. The *ROSAT* HRI, thanks to its smaller positional uncertainty, would have been a better choice for the selection of blanks, but no HRI catalogs were available when this project was initiated.

This gave 81 sources. After visual inspection 10 of these sources proved to be false due to limitations of the detection algorithm: there can be false detections near bright sources or detections close to the inner circle boundary due to the spread of a bright source falling in the outer circle. The final sample is thus composed of 71 sources.

However careful inspection showed that some of the 71 *ROSAT* fields had WGACAT coordinates not in agreement with other position estimates and in some cases the displacement was larger than the $26''$ radius error circle used for the cross-correlation. Some of our blanks had no optical counterparts because of the wrong X-ray positions. This shift in WGACAT coordinates is related to an error in converting the header of the old format event files into RDF format; this error caused an offset in the source declination up to $1'$. These problems were solved in the newly released Revision.2 *ROSAT* PSPC data, available in the HEASARC database.

3.1. Revised Sample

In order to quantify how many sources had WGACAT coordinates with an offset $\geq 26''$ we used the incomplete Galpipe catalog (Fabbiano et al. in preparation) and found improved Revision.2 coordinates for 54 of the 71 objects (76% of the sample). Out of these, 39 had a shift between WGACAT and Galpipe positions smaller than $26''$. (Note that even if $\sim 30\%$ of the sources in our sample have an offset $> 26''$ only 431 observations out of 3644 ($\sim 12\%$) in WGACAT were affected by this problem.) Our method was highly efficient at selecting coordinate errors, as well as true ‘blanks’. Since no *ROSAT* PSPC catalog based on Rev.2 images was completed at that time⁶, it was not possible to perform the whole selection using the correct coordinates. We repeated the cross-correlations with the POSS using the Galpipe coordinates of the 54 WGACAT-Galpipe sources using a more conservative $39''$ radius error circle, corresponding to 3σ confidence (Boyle et al. 1995). We have been left with the 16 blank field sources listed in Table 1. As a result of this change in definition, our sample is not statistically complete.

Note also that clearly X-ray bright sources could still have high $f_X/f_V > 10$ and not be included in our sample if their optical counterpart exceeds the $O > 21.5$ limit.

4. ROSAT DATA ON BLANK FIELD SOURCES

We searched the *ROSAT* archive for all PSPC and HRI observations of the final sample of the 16 ‘blanks’ listed in Table 1. Besides the PSPC observations used for the selection, six ‘blanks’ have other serendipitous detections in both the PSPC and HRI. A list of all the *ROSAT* observations is presented in Table 2.

To determine the rough X-ray spectral properties of our blanks we measured their X-ray hardness ($HR=H/M$) and softness ($SR=S/M$) ratios based on the WGACAT95 count rates in the standard *ROSAT* PSPC bands: Soft, S (0.1-0.4 keV), Medium,

⁴Since the sliding cell algorithm is sensitive to point sources, it can find spurious sources where extended emission is present. WGACAT includes a quality flag, DQFLAG, that notes dubious detections based on a visual inspection of the fields.

⁵ $\sim 36-74\%$ when using the $39''$ 3σ radius error circle (see below).

⁶A second version of the WGACAT based on rev. 2 data was released on May 20, 2000 (WGACAT00). On the same day an updated version of WGACAT95 was released. The positional problem in WGACAT95 was solved thanks to our note to the authors (Cagnoni, White, Giommi & Angelini 1998, private communication).

M (0.4–0.86 keV), and Hard, H (0.87–2 keV). We converted these ratios into effective X-ray spectral indices α_S (0.1–0.8 keV) and α_H (0.4–2.4 keV), to correct for the variable Galactic line-of-sight absorption, and the energy-dependent PSF, following Fiore et al. (1998). Note that the effective spectral indices are not physical spectral slopes, but should be considered analogous to U-B and B-V colors, (see Fiore et al. 1998 for a detailed discussion). Due to the low signal-to-noise ratio of X-ray data, individual spectral indices are not reliable but they are useful on a statistical basis.

In Figure 1 we compare the effective spectral indices of the blanks (filled circles) with (a) those of a sample of radio-quiet quasars and (b) of a sample of radio-loud quasars from Fiore et al. (1998), as they derive the effective spectral indices in the same way and using the same correction factors to the WGA-CAT hardness ratios. Blanks tend to have harder spectra, both in the soft and hard PSPC bands, when compared to the radio-quiet quasars, while their distribution is closer to that of the radio-loud ones. Could this be due to a radio-loud nature for the blank field sources? This is not confirmed by radio data (§ 6).

We simulated the spectra of the main classes of X-ray sources to find their place in the $\alpha_S - \alpha_H$ plane (Figure 1). We modeled stars using a black body spectrum; for $kT \leq 70$ eV they have steep PSPC spectra with $\alpha_S \geq 2$ and $\alpha_H > 4$, and thus would fall outside of the region plotted in Figure 1 in the upper right corner direction. To simulate normal galaxies and local clusters of galaxies we used a Raymond-Smith thermal spectrum with the temperature ranging from 1 to 10 keV. Such sources lie in a region with $-0.7 \leq \alpha_S \leq 0.2$ and $0 \leq \alpha_S \leq 0.7$. For $kT \sim 1$ keV local groups and clusters are thus expected to contaminate the blank field sources falling below the diagonal line in Figure ??b. Increasing the temperature would shift them down in the plot parallel to the diagonal line and out of the region occupied by the blanks. We also simulated Seyfert-2s with an absorbed power law model ($N_H = 10^{21} \text{ cm}^{-2}$ and 10^{22} cm^{-2}). As absorption cuts-off their low energy spectra, Seyfert-2s lie in the $\alpha_S < \alpha_H$ region of the diagram: for $N_H = 10^{21} \text{ cm}^{-2}$ near the highest temperature local clusters (below the diagonal line at $\alpha_H \sim 0$); increasing the N_H makes them shift out of the plotted region on a diagonal path. The BL Lac spectral shape depends on the position of the SED peaks with respect to the X-ray band: we adopt a simple power law model with $\alpha_S = \alpha_H$ (diagonal line in Figure 1) as a good representation (e.g. Maraschi et al. 1995; Urry et al. 1996).

4.1. PSPC X-ray Spectra

We extracted the spectra of the 16 blanks from the archival Revision.2 ROSAT PSPC data at HEASARC using XSELECT 2.0. When the source was detected in more than one observation we combined the spectra. We used as source extraction region a circle with a radius of 160 pixels (1'20'') and as background an annular region centered on the object (radii 1.6–3.2') from which we removed any obvious sources. We fit the PSPC spectra of each source using XSPEC 11.0.1 with three different models:

- (1) an absorbed power law model of the form

$$F(E) = k \times E^{-\Gamma} \exp[-N_H \sigma_H]$$

where $F(E)$ is in photons $\text{cm}^{-2} \text{ s}^{-1} \text{ keV}^{-1}$, Γ is the photon index, k is the normalization at 1 keV and the (local) absorption is

characterized by a column density N_H and an absorption cross section σ_H . We fitted the data leaving all the parameters free and again fixing the absorbing column to the Galactic value from the Bell Labs HI survey (Stark et al. 1992, found with *w3nh* at HEASARC).

The fit values of Γ and N_H are plotted for each source in Figure 2. As evident in Figure 2 the power law fit gives a $\geq 3\sigma$ indication, for an absorbing column in excess of the Galactic value for three blank field sources (filled points in Figure 2). It appears that, omitting three sources with high Galactic N_H ($> 4.26 \times 10^{20} \text{ cm}^{-2}$), the spectra fall into two groups:

- (a) - the ‘absorbed’ sample: sources with an indication of absorption in excess of the Galactic value ($\alpha_H \leq 0.62$ and $\alpha_S \leq 0.70$), including three sources (1WGA J1243.6+3204; 1WGA J1216.9+3743 and 1WGA J0951.4+3916);
- (b) - the ‘unabsorbed’ sample: sources with absorption consistent with the Galactic value ($\alpha_H > 0.62$ and $\alpha_S > 0.70$).

- (2) an absorbed black body model of the form

$$F(E) = k \times 8.0525 E^2 dE / ((kT)^4 (\exp(E/kT) - 1)) \exp[-N_H \sigma_H]$$

where k is the normalization and kT is the temperature in keV. 1WGA J1243.6+3204 and 1WGA J1216.9+3743 still require high absorption, while 1WGA J0951.4+3916 is consistent with the Galactic value.

- (3) an absorbed optically thin thermal plasma (Raymond & Smith, 1977) with absorption fixed to the Galactic value, abundances fixed to 0.1 times the Solar value and redshift free to vary between 0 and 2.

The results of these fits are reported in Table 3 and the spectra of the blanks fitted with the absorbed power law model and their residuals are reported in Figure 3.

The spectra of the individual sources do not have enough statistics to discriminate between the competing models.

4.1.1. Combined spectra

In order to gain statistics, we computed the average spectra of these two groups of absorbed and unabsorbed sources (Figure 4). We sub-divided the unabsorbed sources into two groups, i.e. the sources observed before and after the change in the PSPC gain occurred on October 1991, computed two separate combined spectra and then fitted the two spectra simultaneously. All the sources in the absorbed sample were observed after October 1991.

By fitting these composite spectra with the models described in § 4.1, we obtained the results summarized in Table 3. The best fit model for both samples is an absorbed power law with photon index ~ 2 . The ‘absorbed’ sample requires $N_H \sim 2 \times 10^{21} \text{ cm}^{-2}$, well in excess of the Galactic value, while for the ‘unabsorbed’ sample a Galactic column density is acceptable. The Raymond-Smith model provides a good description of the data for both the unabsorbed and absorbed (once the column density is left free to vary) sample. The black body model is acceptable for the ‘absorbed’ sample, but it completely fails to describe the ‘unabsorbed’ sources. The large χ^2 values obtained for the ‘unabsorbed’ sample suggests a more complex spectral shape, probably because different classes of sources are involved.

4.2. X-ray fluxes

We computed the absorbed X-ray fluxes in the 0.5-2.0 keV (the standard *ROSAT* band), 0.05-2.5 keV (the WGACAT95 band) and 0.3-3.5 keV (*Einstein* band) using the best fit absorbed power law model for each source (with the free absorption value, except for 1WGA J1103.5+2459, for which freeing the absorption leads to a value ~ 4 time smaller than the Galactic value). The results are reported in Table 4.

For 4 sources (1WGA J1416.2+1136, 1WGA J1535.0+2336, 1WGA J1103.5+2459 and 1WGA J1415.2+4403) the 0.3-3.5 keV flux we estimated is $\sim 40\%$ lower than the WGACAT95 flux. Since $f_X(0.3 - 3.5\text{keV}) < 10^{-13} \text{ erg cm}^{-2} \text{ s}^{-1}$ for these sources, their f_X/f_V is less extreme and compatible with normal type 1 AGNs. However this discrepancy is due to a steep (for 1WGA J1416.2+1136, 1WGA J1103.5+2459, and 1WGA J1415.2+4403) or a flat spectral slope (1WGA J1535.0+2336) compared to the average type 1 AGN spectrum for which the WGACAT count rate-to-flux conversion factor was estimated. Instead five sources (1WGA 0432.4+1723, 1WGA 1220.3+0641, 1WGA 1226.9+3332, 1WGA 1233.3+6910 and 1WGA J1340.1+2743) have larger f_X than in the WGACAT. With $f_X(0.3 - 3.5\text{keV}) > 4 \times 10^{-13} \text{ erg cm}^{-2} \text{ s}^{-1}$ and lack of a POSS counterpart, their f_X/f_V is not even compatible with extreme BL Lacertae objects.

4.3. Variability

We extracted the lightcurves for sources and backgrounds (using the same regions chosen for the spectral analysis) within each PSPC and HRI observation. We binned the lightcurves with bin sizes ranging from 1000 s to 5000 s and calculated the maximum variation factor of the count rate considering the points with errorbars smaller than 40%. The average maximum variability factor is 1.60 ± 0.71 , consistent with the sources being constant. The variability factor was computed using all the available lightcurves spanning a minimum time scale of 1ks to a maximum time scale of ~ 2 years. No strong variability is seen. Neither do we see variability when comparing multiple PSPC and/or HRI observations, for the 10 sources with multiple observations: the count rates are consistent, within the large errors due to spectral uncertainties.

We also searched the RASS and three blanks were detected in 1990 (Table 5); all of them have RASS count rate consistent within 1σ with the pointed observations except for 1WGA J1233.3+6910, whose measured count rates can be reconciled within 2σ (a factor 1.6 variability; Table 5). An extremely variable nature, transient or burst-like, is excluded for all the 16 blanks.

4.4. ROSAT HRI: extent

7 sources have one or more *ROSAT* HRI observations (see Table 2). Only one source (1WGA J1216.9+3743) is not visible in the HRI images. The detected sources look pointlike. 1WGA J1226.9+3332 (§ 7.4) has an extension at the limit of the HRI PSF ($\sim 5''$) and looks extended in a *Chandra* follow-up observation (Cagnoni et al. 2001b). 1WGA J1233.3+6910, instead, falls on the detector's edge making any estimate of count rate, position and extent unreliable. The HRI positions and count rates are reported in Table 1.

⁷We used NVSS fluxes instead of FIRST fluxes because the latter ones can be underestimated because of the high spatial resolution of the survey. Even in the NVSS, some of the flux coming from extended sources could be either resolved out or split into two or more components, leading to a systematic underestimate of the real flux densities of such sources (Condon et al. 1998).

5. ASCA

We searched the ASCA public archive for serendipitous observations of the 16 blanks and we found that 4 of them (1WGA J1226.9+3332, 1WGA J1535.0+2336, 1WGA J1415.2+4403 and 1WGA J1220.3+0641) fall in the ASCA GIS field of view (see the log in Table 6). All the sources but 1WGA J1415.2+4403 are detected, but 1WGA J1226.9+3332 and 1WGA J1535.0+2336 are too faint to derive spectra. For 1WGA J1220.3+0641, instead, ASCA data provide valuable broad X-ray spectral information. The results are discussed in the sections dedicated to each source (§ 7).

6. RADIO

To check on the radio emission of the blanks we searched for radio counterparts in the NRAO VLA Sky Survey (NVSS, Condon et al. 1998) and in the FIRST survey (Becker, White & Helfand 1995) within the $39''$ X-ray error circle. Both surveys were conducted at 1.4 GHz. The NVSS has a limiting flux of ~ 2.5 mJy and a position uncertainty of few arcseconds. The FIRST ongoing survey reaches ~ 1 mJy with a position accuracy $< 1''$. We found 4 NVSS counterparts for the blanks, 2 of which detected also in the FIRST. The remaining 2 NVSS sources are in an area not yet covered by FIRST (see Table 7). We computed the broad band spectral indices α_{ro} and α_{ox} (similar to f_X/f_V) for the 4 sources with radio data using the NVSS radio flux, the X-ray flux at 1 keV (see Table 3) and a O magnitude limit of 21.5 (considered to be equal to the V magnitude).⁷

For 1WGA J1226.9+3332, identified as a $z=0.89$ cluster of galaxies (see § 7.4) we measured a R band magnitude of 20.4 and we converted it into V magnitude of 22.2 using $(V-R)=1.83$, typical for an elliptical galaxy at $z=0.89$ (Coleman, Wu & Weedman 1980), obtaining $\alpha_{ro} = 0.60$ and $\alpha_{ox} = 0.68$. For 1WGA J1340.1+2743, a BL Lac (see § 7.1) we used $R \sim 22$ (from Lamer, Brunner & Stauber 1997) and converted it using the mean $V - R \sim 0.65$ found for BL Lacs (Moles et al. 1985) and we obtained $\alpha_{ro} = 0.63$ and $\alpha_{ox} = 0.61$. Both sources are radio-loud with $f_{(1.4\text{GHz})}/f_V \sim 1000$.

For the remaining two blanks with a radio counterpart we obtained values of $\alpha_{ro} \geq 0.5$ and $\alpha_{ox} \leq 0.7$.

We also translated the f_X/f_V ratio into α_{ox} for the remaining sources.

Since BL Lacs are the known class of X-ray emitting sources with higher f_X/f_V , we compared the α_{ro} , α_{ox} with those of X-ray selected BL Lacs (e.g. Caccianiga et al. 1999). Figure 5 shows that the blanks with a radio counterpart occupy an extreme region of the $\alpha_{ro}-\alpha_{ox}$ plane, where just few BL Lac objects fall. Deeper radio observations would be of great value.

7. DISCUSSION AND NOTES ON INDIVIDUAL SOURCES

In this section discuss all the possibilities for the blanks nature presented in § 2. This section also includes all the available information on the sources at the time of writing. While all of them were unidentified when the sample was first selected, some were studied (and in some cases identified) by other groups while we were progressing with the investigation. A schematic summary of the identified sources and a possible classification for the still unidentified ones is presented in Table 8.

7.1. BL Lacertae objects

1WGA J1340.1+2743

1WGA J1340.1+2743 was observed 7 times with the PSPC, only once in the inner circle. We extracted a combined image and spectrum. This source is close ($\sim 7'$) to the bright Seyfert 2 galaxy CC B00 (1RXS J134021.4+274100) which has ~ 2 times 1WGA J1340.1+2743 count rate. Due to slight displacements in the source positions as detected in different images and to the broader PSF in the outer regions of the detector, 1WGA J1340.1+2743 is contaminated by the nearby bright source making the combined image not suitable for variability or flux estimates.

1WGA J1340.1+2743 was identified as a BL Lac in Lamer, Brunner & Staubert (1997) because of lack of spectral features in its optical spectrum. Lamer et al. find an X-ray flux at 1 keV of 2.06×10^{-14} erg cm $^{-2}$ s $^{-1}$. In a ROSAT observation during which the source falls in the PSPC outer rim. This value is 50% smaller than the 3.07×10^{-14} erg cm $^{-2}$ s $^{-1}$ we find for the detection in the inner PSPC circle. 1WGA J1340.1+2743 has a radio counterpart $\sim 10''$ from the PSPC position (see § 6 and Table 7). However the $\alpha_{ro} = 0.62$ and $\alpha_{ox} = 0.61$ (see § 6 for details) and the $f_x/f_v \sim 300$ are not compatible with the values of ‘normal’ BL Lacs. An extreme BL Lac (e.g. Costamante et al. 2001) with the synchrotron peak lying, at energies higher than the ROSAT band, could fit this source. The X-ray spectral slope ($\Gamma = 2.35 \pm 0.18$) is also similar to those found with *Beppo-SAX* by Costamante et al. (2001) for extreme BL Lacs.

Another possibility is that 1WGA J1340.1+2743 is an ‘average’ X-ray selected BL Lac, that was undergoing a large flare during the WGACAT95 detection: a factor of 10-30 variation has been observed in X-ray selected BL Lacs (e.g. MRK 501, Pian et al. 1998) and a 10 times smaller ‘quiescent flux’ would drastically lower the f_x/f_v down to ~ 20 , a normal value for BL Lacs. This hypothesis, however, is not confirmed by the PSPC lightcurve, where no dramatic changes in the X-ray flux are visible other than a factor of 2 brighter with respect to the results by Lamer, Brunner & Staubert (1997).

7.2. Isolated neutron stars

As mentioned in §2.2, the spectrum expected from INSs is thermal, with typical temperatures $T \sim 100$ eV (but models with harder spectra have also been proposed, e.g. Zampieri et al. 1995). The flat spectra of blanks suggests that statistically it is unlikely that they are INSs, even though INSs could hide among the softest sources in our sample. With a well-defined statistical sample it will be possible to set limits on the surface and space density of INSs.

7.3. The AGNs and AGNs candidates

1WGA J1220.3+0641

1WGA J1220.3+0641 was detected in the RASS and it is listed in the Bright Source Catalog (BRASS, Voges et al. 1999) with a broad band $CR = 0.079 \pm 0.017$ counts s $^{-1}$. Using the whole 0.07- 2.4 keV ROSAT band we derive a $CR = 0.098 \pm 0.006$ counts s $^{-1}$ consistent with the RASS detection. Its position in the BRASS catalog is $14''$ from the Galpipe position and $10''$ from the HRI position. The HRI and Galpipe positions for this source are only $4''$ apart.

ASCA found 1WGA J1220.3+0641 as an unidentified serendipitous source in 1995 in the ASCA GIS with a 1-10 keV count rate of 0.0142 ± 0.0009 (George et al. 2000). This source is also included in the ASCA Medium Sensitivity Survey (AMSS)

(Ueda et al. 2001) with the name 1AXG J122017+0641. The ASCA archival lightcurves do not show any strong variability (Figure 7). In the AMSS the source has a count rate of 0.0214 counts s $^{-1}$ in the 0.7-7.0 keV band, corresponding to a flux, corrected for the Galactic absorption, of 1.4×10^{-12} erg cm $^{-2}$ s $^{-1}$, with most of the flux lying in the 2-10 keV band. An absorbed power law model with absorption fixed to the Galactic value (1.56×10^{20} cm $^{-2}$) well describes the source; while freeing the absorption does not improve the fit. ASCA GIS2 and GIS3 data give values of $\Gamma = 1.31 \pm 0.58$ and normalization of 4.16×10^{-4} photons cm $^{-2}$ s $^{-1}$ keV $^{-1}$ at 1 keV, with a reduced χ^2 of 0.79 (33 d.o.f.). The simultaneous fit of ROSAT PSPC and ASCA GIS2 and GIS3 spectra gives a best fit photon index of 1.18 and a normalization of 3.38×10^{-4} photons cm $^{-2}$ s $^{-1}$ keV $^{-1}$ at 1 keV, with a reduced χ^2 of 2.608 (56 d.o.f.). The data and the unfolded spectra fitted with an absorbed power law model are presented in Figure 6.

If the absorbed power law is a correct model, 1WGA J1220.3+0641 looks like a normal type 1 AGN.

The POSS shows the presence of a O=21.81 and E=18.58 red source within the 1WGA J1220.3+0641 error circle. A local source with O-E=3.23 would be strongly obscured ($A_V \sim 6$) if an intrinsic quasar spectral shape (e.g. Francis et al. 1991) is adopted (e.g. Figure 7 in Risaliti et al. 2001).

1WGA 1412.3+4355

This source has been classified as an AGN at $z \sim 0.59$ in the RIXOS survey (Mason et al. 2000) on the basis of one broad optical emission line identified with Mg II. The RIXOS (0.5 - 2.0 keV) count rate is 0.0055 ± 0.006 counts s $^{-1}$, compatible with our measurement. The X-ray photon spectral slope we find is 2.02 ± 0.15 (c.f. 2.1 ± 0.1 in the RIXOS) consistent with a normal type 1 AGN and the spectrum does not show signs of an absorbing column in excess of the low Galactic value (1.17×10^{20} cm $^{-2}$). 1WGA 1415.2+4403 is not variable in the PSPC observation, but there are no other observations for this source.

The POSS shows a E=18.73 source within the error circle, but no objects are detected in the O-band; assuming a limit of O>21.5, we obtain a color of O-E> 2.77, corresponding to $A_V > 4$ at $z = 0.59$ for a quasar.

1WGA 1415.2+4403

1WGA 1415.2+4403 is also included in the RIXOS survey (Mason et al. 2000) and classified as a $z = 0.562$ AGN based on 3 optical lines. The RIXOS (0.5 - 2.0 keV) count rate is 0.0033 ± 0.0005 counts s $^{-1}$, comparable to our count rate (0.0030 ± 0.0006 counts s $^{-1}$). The photon spectral slope is $2.70^{+0.22}_{-0.20}$ (2.3 ± 0.1 in the RIXOS) steeper than typical type 1 AGNs. There are no signs of absorption in the X-ray spectrum. This source is not variable in the PSPC observation.

1WGA 1415.2+4403 was serendipitously observed by the ASCA satellite in 1996 (Table 6) but the source was not detected. The 3σ upper limit on the GIS2+GIS3 count rate in a $r = 6''$ circle is 0.00155 counts s $^{-1}$, consistent with the count rate predicted by PIMMS by extrapolating the ROSAT PSPC count rate using the best fit power law with Galactic absorption (values taken from Table 1 and Table 3).

No sources are found in the POSS O and E bands within the X-ray error circle. We note that the WGACAT95 flux was $\sim 50\%$ overestimated (see §4.2 This source is, as a consequence, one of the least extreme in our sample; the f_x/f_v is ~ 5 and f_x/f_R (Hornschemeier et al. 2001) ~ 1 are both consistent with the tail of normal type 1 AGNs.

1WGA J1416.2+1136

This source was found in the Cambridge ROSAT Serendipitous Survey (CRSS, Boyle, Wilkes & Elvis 1997) with a (0.5–2.0 keV) X-ray flux of 5.2×10^{-14} erg cm $^{-2}$ s $^{-1}$ implying a count rate of 0.433×10^{-2} counts s $^{-1}$, larger than our count rate of $(0.31 \pm 0.08) \times 10^{-2}$ counts s $^{-1}$. In the ROSAT HRI the count rate is consistent with PIMMS estimates based on the PSPC count rate suggesting a constant source over a 4-year period. Also for this source the WGACAT was overestimated ($\sim 60\%$) and the source is thus less extreme than previously thought. The X-ray photon spectral index is $2.68^{+0.27}_{-0.24}$, somewhat steep for a normal type 1 AGN.

On the POSS there is a O=22.22 and E=19.50 source 12.8'' from the HRI position. The redness of the source O-E=2.72 implies $A_V \sim 5$ for a typical AGN spectrum (Francis et al. 1991), corresponding to $N_H \sim 10^{22}$ cm $^{-2}$. The ROSAT spectrum, however, is consistent with Galactic absorption.

1WGA J1535.0+2336

This source was detected by the *Einstein* IPC as an ultra-soft source (Thompson, Shelton, & Arning 1998) with a count rate of $(3.64 \pm 0.96) \times 10^{-3}$ counts s $^{-1}$, in good agreement with the PSPC count rate using our best fit values for an absorbed power law model (Table 3). The *Einstein* and Galpipe positions are 17'' apart and thus consistent. The X-ray spectral slope ($\Gamma = 0.70^{+0.72}_{-1.05}$) is consistent within the large errorbars with a type 1 AGN. 1WGA J1535.0+2336 was detected in 1993 by the ASCA GIS (Table 6) with a full band GIS2+GIS3 count rate of $\sim (8 \pm 3) \times 10^{-4}$ counts s $^{-1}$ in a $r = 2.25'$ radius circle. An extrapolation of the ROSAT PSPC count rate into the ASCA band using the flat best fit spectral slopes ($\Gamma = 0.7$ for a power law model with free absorption) overestimates the ASCA count rate by about an order of magnitude. A steeper value, $\Gamma = 2.2$, which still lies within the 2σ uncertainty on the ROSAT fit, is needed to achieve consistency with ASCA and with the *Einstein* ultra-soft ($\Gamma > 2$) nature. This is a typical value for type 1 AGNs. A ~ 2 days timescale variability (the time distance between the ROSAT and ASCA observations) could also reconcile the measured count rates.

1WGA J1535.0+2336 has an extremely flat spectral slope and the AGN-like count rate to flux conversion used in the WGACAT95 gives a $\sim 90\%$ overestimated flux value. A O=21.79 and E=19.61 source is visible in the Palomar within the 1WGA J1535.0+2336 error circle. O-E=2.18 implies $A_V \sim 4$ for a local source and $N_H \sim 8 \times 10^{21}$ cm $^{-2}$ (assuming Galactic dust to gas ratio), while the X-ray fit does not show the need for extra absorption.

7.3.1. Discussion on the blank field AGNs

When we started this project we expected to find examples of peculiar AGNs such as absorbed ones (QSO-2s or LMSy2s) or low efficiency radiators (§ 2). Indeed two sources, 1WGA J1412.3+4355 and 1WGA J1415.2+4403 were spectroscopically identified in the RIXOS survey (Mason et al. 2000) as AGNs and while the latter could be a normal type 1 AGN (see § 7.3), the first one has an unexpected Palomar counterpart (see § 7.3). Another 5 sources (1WGA J1220.3+0641, 1WGA J1416.2+1136, 1WGA J1535.0+2336, 1WGA J1233.3+6910 and 1WGA J0951.4+3916, see Table 8) are likely to be AGNs. 1WGA J0951.4+3916 stands out because it shows signs of absorption in the X-ray band ($N_H \sim 2^{+3}_{-1} \times 10^{21}$ cm $^{-2}$, Table 3) and has a red source in the POSS E-band (E=19.1).

The remaining 4 AGN-like sources seem to share the same peculiar combination of characteristics: they have X-ray spectra typical of type 1 AGNs ($\Gamma \sim 2$ and absorbing column densities consistent with the Galactic values (except for 1WGA J0951.4+3916 which shows an X-ray derived $N_H \sim 2 \times 10^{21}$ cm $^{-2}$) and they have red (O-E > 2) counterparts in the POSS E-band at $E < 19.5$ (Table 8) (with the exception of 1WGA J1415.2+4403). For a local AGN type 1, $O-E > 2$ implies $A_V > 4$ (e.g. Risaliti et al. 2001) and thus strong obscuration ($N_H > 2 \times 10^{21}$ cm $^{-2}$ for a dust to gas ratio typical of the ISM in our Galaxy), in contrast to the results of the X-ray data. Since the host galaxy is not visible, we can assume $z \geq 0.2$ for the AGN blanks; this implies $L_{X(0.3-3.5\text{keV})} > 7.5 \times 10^{42}$ erg s $^{-1}$ or a bolometric X-ray luminosity $L_X \sim 3.7 \times 10^{44}$ erg s $^{-1}$ for a type 1 AGN (and a total mass $> 3 \times 10^6 M_\odot$) which is too bright for the galaxy emission to be important. We propose here some possibilities to reconcile X-ray and POSS data.

High redshift

As is clear from Figure 7 of Risaliti et al. (2001), at $z \geq 3.5$ AGNs have $(O-E) > 2$, even for the low Galactic A_V . The X-ray luminosity of the blanks if they were at $z \sim 4$ would be $\geq 10^{47}$ erg s $^{-1}$, consistent only with a quasar. This option would be excluded for the two sources spectroscopically identified in the RIXOS (1WGA J1412.3+4355 and 1WGA 1415.2+4403), which have $z \sim 0.5-0.6$ (Mason et al. 2000), but while for one of these (1WGA 1415.2+4403) the 3 observed optical lines uniquely determine the redshift, for 1WGA J1412.3+4355 the redshift is uncertain. In fact only one optical line at ~ 2800 Å was observed and identified as Mg II; if the observed line were instead the Ly α line (1216 Å rest frame), the redshift of the source would be 2.66, almost in agreement with the Palomar color of the counterpart.

High dust to gas ratio

Another way to reconcile the lack of absorption in the X-rays (mainly due to neutral hydrogen) with the obscuration in the optical band (due to dust) suggested by the red POSS counterparts, is to assume an higher than Galactic dust to gas ratio. We derived the A_V for the 4 sources with a counterpart in the POSS E band using the colors in Table 1 and Figure 7b of Risaliti et al. (2001) assuming a local redshift, except for the two RIXOS AGNs with measured redshifts. We then derived the A_V/N_H using the Galactic N_H for each source (Stark et al. 1992) and compared it to the extrapolation of the expected variation of the A_V/N_H ratio as a function of the dust-to-gas ratio presented in Maiolino et al. (2001a) (their Figure 2). We derive dust to gas ratios $\sim 40-60$ times the Galactic value when Solar metallicity is assumed. Observational evidence however shows a tendency of AGNs to have lower than Galactic dust to gas ratios (e.g. Maccacaro, Perola & Elvis 1982; Risaliti et al. 2001; Maiolino et al. 2001b). Furthermore such high dust to gas ratio is physically difficult to justify: in fact, assuming a Galactic dust to gas ratio $\sim 1\%$ ($M_{\text{gasGal}} = 8 \times 10^9 M_\odot$, Zombeck 1990 and $M_{\text{dust}} \sim 10^7 M_\odot$ for spiral galaxies, Block et al. 1994) the dust to gas ratio needed to reconcile Palomar and X-ray absorptions implies $\sim 40-60\%$ of dust to gas ratio, a value exceeding the $\sim 37\%$ of giant stars, the most efficient sources of dust formation in the Universe (Whittet 1992).

Maiolino et al. (2001b) find an higher than Galactic ratio for low luminosity objects ($L_X \sim 10^{41}$ erg s $^{-1}$) and suggest that these may be physically different from the more luminous “classical” AGNs. We explore this option later in this section.

⁸Using a constant conversion factor of 1 count s $^{-1} = 1.2 \times 10^{-11}$ erg cm $^{-2}$ s $^{-1}$

A different grain size distribution

A possibility that cannot be excluded is a modified dust grain size distribution with respect to the Galactic diffuse ISM (Mathis, Rumpl & Nordsieck 1977). A strong dominance of small grains would increase the optical extinction without significant modifications of the X-ray absorption.

A dusty warm absorber

AGN with a lack of X-ray absorption and the presence of optical obscuration have been detected previously (e.g., Brandt, Fabian & Pounds 1996; Komossa & Fink 1997). The solution favored for these objects is the presence of dusty ionized absorbers. In this model the dust is located within the ionized material and no X-ray cold absorption is detected. The presence of dust within the warm absorber is expected to flatten the X-ray spectrum (Komossa & Bade 1998), but we note that the slope range of the blanks AGNs(candidates) ($\Gamma = 0.70 - 2.97$) is consistent with the sources for which a dusty warm absorber was proposed (e.g. IRAS 13349+2438: $\Gamma = 2.81$, Brandt et al. 1996; NGC 3227: $\Gamma = 1.19$, Komossa & Bade 1998; NGC 3786: $\Gamma = 1.0$, Komossa & Fink 1997).

Missing or shifted BBB

Galaxies with bright X-ray emission ($L_X \sim 10^{42} - 10^{43}$ erg s $^{-1}$) but weak or absent AGN features in the optical band have been known to exist since *Einstein* observations (Elvis et al. 1981; Tananbaum et al. 1997), and are now being found in large numbers (e.g. Della Ceca et al. 2001; Hornschemeier et al. 2001, Fiore et al. 2001; Comastri et al. 2002). A way to explain the faintness of the optical counterparts for these sources and for the five AGN-like blanks is to assume that the AGN is intrinsically optically faint.

The intrinsic faintness could be related to a highly suppressed BBB emission. Such suppression happens in low radiative efficiency accretion (§ 2).

To check if this is consistent with the extreme properties we observe in our blanks we derived the V magnitude and the α_{ro} and α_{ox} from the spectral fit to Sgr A* (Figure 1 of Narayan et al. 1998), assuming a distance of ~ 10 kpc.⁹ We derive $\alpha_{ro} \sim 0.61$, $\alpha_{ox} \sim 1.12$ and $f_X/f_V \sim 18$, which are compatible with blank field sources. These values are only indicative as could readily be made more extreme by changing the parameters of the model. If blanks are such systems, the low accretion rate, coupled with the observed luminosity ($L_X \geq 3.7 \times 10^{44}$ erg s $^{-1}$ at $z \geq 0.2$) implies a large mass ($M \geq 3 \times 10^9 M_\odot$).

The BBB emission may appear to be suppressed if its peak is shifted out of the optical band, as for low mass black holes. High energy BBB have been already observed (e.g. in the NLSy RE J1034+396, Puchnarewicz et al. 1995; 2001). Even though we cannot exclude such a possibility, we note that this option does not hold for the X-ray bright, optically dull galaxies (e.g. Comastri et al 2002): even if shifted, the BBB emission would still provide the photons necessary to ionize hydrogen and show characteristic AGN emission lines which are not detected. Furthermore, if the most extreme blanks were nonvariable NLSy, an higher f_X/f_V would imply higher disk emission and thus an unlikely higher accretion rates (NLSy are already thought to accrete close to the Eddington limit, e.g. Laor et al. 1997, Leighly 1999, Turner et al. 1999 and references therein).

Extremely variable AGNs

⁹We get $f_{(1.4\text{GHz})} = 580$ mJy, $V=17.22$ and $f_{(1\text{keV})} = 7.75 \times 10^{-4}$ photons cm $^{-2}$ s $^{-1}$ keV $^{-1}$, while the 0.3-3.5 keV flux is $\sim 10^{-11}$ erg cm $^{-2}$ s $^{-1}$ ($L_{(0.8-2.5\text{keV})} = 1.55 \times 10^{34}$ erg s $^{-1}$ Narayan et al. 1998)

None of the sources seems to be extremely variable within each PSPC or between different observations, but we cannot a-priori exclude a high X-ray state during the *ROSAT* observations.

7.4. Clusters of galaxies

1WGA J1226.9+3332

This source is listed in Radecke (1997). Using the same PSPC data, he found a count rate of 2.20×10^{-2} counts s $^{-1}$ slightly smaller than ours, $(2.66 \pm 0.16) \times 10^{-2}$ counts s $^{-1}$. Short term variability is not visible between the PSPC observations taken two weeks apart. In the HRI image the source is faint with a count rate of $(8.7 \pm 1.5) \times 10^{-3}$ counts s $^{-1}$, in agreement with PIMMS predictions based on the PSPC observations, indicating a non-variable source over a 4-year period. The HRI image is not conclusive for extension information. We obtained a 10 ks Cycle 1 *Chandra* observation for 1WGA 1226.9+3332 (Cagnoni et al. 2001a) confirming the high z ($z=0.89$) cluster nature of this blank (see also Ebeling et al. 2001). 1WGA J1226.9+3332 was also serendipitously detected in 1998 and in 2000 by the ASCA GIS. The source falls at the border of the useful area of the GIS2 and GIS3 detector and its count rate (GIS2+GIS3 full band count rate = 0.0038 ± 0.0005 count s $^{-1}$) should be considered a lower limit, but it probes to be close to the expected one. (based on a PIMMS simulation with a Raymond-Smith model with $kT = 10$ keV and absorption fixed to the Galactic value).

1WGA J0221.1+1958

1WGA J0221.1+1958 was identified in the SHARC survey (Romer et al. 2000) as a $z = 0.45$ cluster of galaxies, and assuming a $kT \sim 6$ keV, they derived from a *ROSAT* count rate of 0.02211 counts s $^{-1}$ an X-ray luminosity of $L_{X(0.5-2.0\text{keV})} = 2.87 \times 10^{44}$ erg s $^{-1}$ ($H_0=50$ km s $^{-1}$ Mpc $^{-1}$ and $q_0 = 0.5$).

1WGA J0432.4+1723

This source was found by Carkner et al. (1996) in the outer PSPC region (offset $\sim 37'$) of a 1993 observation (rp900353n00) of Lynds 1551, a well-studied cloud in the Taurus-Auriga star forming region. They found a 7σ source with count rate of 1.9×10^{-2} counts s $^{-1}$. Even though they do not make a clear identification, the source is included among the sample of possible T Tauri stars. The authors do not find any evidence near 1WGA J0432.4+1723 for $H\alpha$ emission or Li 6707 Å absorption, typical of T-Tauri stars. Moreover the proper motion they measured is inconsistent with the source being part of the cloud. They conclude that 1WGA J0432.4+1723 is likely to be unrelated to the cloud itself. 1WGA J0432.4+1723 was also detected, but not classified, in the analysis of the RASS by Wichmann et al. (1996).

In a 1991 observation, the source falls in the inner PSPC detector region. The ~ 2.5 times longer exposure time and the sharper PSF in the inner circle give more precise results than in Carkner et al. (1996). We find a (0.5-2.0 keV) count rate of $(1.42 \pm 0.1) \times 10^{-2}$ counts s $^{-1}$ and a position (04:32:29.5, +17:23:45.4) consistent with the Galpipe. The fit of the spectrum with a black body model suggests a temperature of $\sim 0.55 \pm 0.01$ keV, somewhat lower than the ~ 1 keV expected for a T Tauri star but not conclusive due to the patchy nature of the ISM in this area. A NVSS radio source with flux equal to 3.2 ± 0.6 mJy is present $\sim 17''$ from the PSPC position. Radio continuum emission is often observed from T-Tauri stars at a level of $10^{15} - 10^{18}$ erg s $^{-1}$ Hz $^{-1}$ and, assuming a distance of

140 pc for L1551, similar to the other Taurus-Auriga star forming clouds (e.g. Carkner et al. 1996), the radio flux corresponds to a luminosity $\sim 10^{17}$ erg s $^{-1}$ Hz $^{-1}$. However the proper motion as reported in Carkner et al. (1996) exclude the possibility of a new T-Tauri star. 1WGA J0432.4+1723 was observed by ROSAT in 1991 and in 1993. The source is persistent and does not show evidence for variability on a 6-hour timescale (the longest timescale sampled, corresponding to the 1991 observation)¹⁰.

1WGA J0432.4+1723 has an E=20.0 Palomar counterpart in its error circle; for $O > 21.5$, the counterpart is at least moderately red ($O - E > 1.5$). We propose a high redshift cluster classification for 1WGA J0432.4+1723 on the basis of the results of follow-up optical and IR imaging observations we performed (Cagnoni et al., in preparation). These observations show the presence of an IR-bright extremely red galaxy in the error circle, and an excess of similarly red sources nearby (see also Cagnoni et al. 2001b, 1WGA J0432.4+1723 is the candidate high z cluster mentioned therein).

1WGA J1103.5+2459

1WGA J1103.5+2459 is listed in Romer et al. (2000) as an extended source detected in the SHARC survey with a (wavelet) count rate of 0.00411 counts s $^{-1}$, but is not identified and is not included in the SHARC cluster sample. This source has a red Palomar counterpart (E=18.2, which implies $O - E > 3.3$) in its error circle and could thus be another high redshift cluster of galaxies.

7.4.1. Discussion on clusters of galaxies

The unabsorbed luminosities of the two high redshift clusters of galaxies we found are high: $L_{X(0.5-2.0)} = 1.28 \times 10^{44}$ erg s $^{-1}$ for 1WGA J0221.1+1958, Romer et al. (2000); and $L_{X(0.5-2.0)} = (4.4 \pm 0.5) \times 10^{44}$ erg s $^{-1}$ for 1WGA J1226.9+3332, Cagnoni et al. (2001a). Since high luminosity, high redshift clusters should be rare, the relative ease with which we discovered them is potentially of great significance. The search for extremely X-ray loud sources can sample a large area of the sky and while the high cut on the sources flux includes the brightest clusters only, the optical cut removes the low z ones. As a result only the few interesting high redshift and high luminosity clusters of galaxies candidates are selected among the $\sim 62,000$ sources in the WGACAT95. With two high z and bright clusters of galaxies already found out of the 16 sources selected in the WGACAT make this method the most efficient way to select these rare sources.

7.5. Ultraluminous X-ray sources in nearby galaxies

1WGA J1243.6+3204

This source was detected by Vogler, Pietsch & Kahabka (1996) in the same observation as the brightest ROSAT source within the optical extent of the edge-on spiral galaxy NGC 4656 ($z=0.00215$). It is located to the south-west, at $\sim 7.6'$ (corresponding to 0.3 kpc at NGC 4656 redshift) from the nucleus along the major axis. In this region there is a deficiency in diffuse, galaxy related X-ray emission, probably due to the cold gas seen in HI which bridges the space between NGC 4656 and its tidally interacting companions (Vogler, Pietsch & Kahabka 1996). These authors estimated a 0.1-2.4 keV count rate of $(9.3 \pm 0.8) \times 10^{-3}$ counts s $^{-1}$, corresponding to $f_X \sim 1.3 \times 10^{-13}$ erg cm $^{-2}$ s $^{-1}$ (0.1-2.4 keV). The N_H value from their fit is in excess of 5×10^{21} cm $^{-2}$, both for a thin thermal plasma and for a

power law model. The absorbing column is larger than the HI density of $\sim 8 \times 10^{20}$ cm $^{-2}$ within NGC 4656 in this direction. There is a 0.3% probability for this blank to be a background X-ray source (Vogler, Pietsch & Kahabka 1996). They also investigate the possibility that 1WGA J1243.6+3204 is a heavily absorbed source within NGC 4656, e.g. a X-ray binary. In this case, $L_X \sim 8 \times 10^{38}$ erg s $^{-1}$ and the source would be radiating well above the Eddington limit for a one solar mass system and need a $10 M_\odot$ black hole to power it. We find a position and a count rate consistent with Vogler, Pietsch & Kahabka (1996). Fitting the spectrum with an absorbed power law in the range 0.07 – 2.4 keV, we find an absorbing column of $1.71^{+1.50}_{-0.78} \times 10^{21}$ cm 2 , clearly in excess of the Galactic absorption ($\sim 1.23 \times 10^{20}$ cm $^{-2}$) and of the column density within NGC 4656 in this direction (8×10^{20} cm $^{-2}$). 1WGA J1243.6+3204 was also serendipitously observed in the ROSAT HRI in a ~ 27 ks long observation performed in 1994, two years after the PSPC one. From the HRI image the source appears pointlike with a more accurate position (12:43:41.1, +32:04:56.6) and a count rate of $(3.4 \pm 0.6) \times 10^{-3}$ counts s $^{-1}$. The HRI and PSPC count rates agree within 1σ .

The same HRI image was also analyzed by Roberts & Warwick (2000) and 1WGA J1243.6+3204 is detected as a serendipitous source with a count rate of $(3.0 \pm 0.4) \times 10^{-3}$ counts s $^{-1}$.

1WGA J1216.9+3743

1WGA J1216.9+3743, as 1WGA J1243.6+3204, lies along the major axis of a nearby galaxy (NGC 4244, at 3.6 Mpc), at $\sim 6'$ (~ 6 kpc) off the galaxy center. 1WGA J1216.9+3743 X-ray emission, as 1WGA J1243.6+3204 one, is strongly absorbed and extremely soft ($\Gamma \sim 5$, see Table 3). 1WGA J1216.9+3743 was not detected by the HRI, as expected from its PSPC count rate. For a *Chandra* observation of this source, which confirms the extremely soft ULX nature, see Cagnoni et al. (2002).

7.5.1. ULX and X-ray binaries discussion

We suggest that these sources could be X-ray binaries in nearby galaxies, as already proposed by Vogler, Pietsch & Kahabka (1996) for 1WGA J1243.6+3204 (see Figure ??). If this is the case, they would be radiating above the Eddington limit for $1M_\odot$ star (unabsorbed $L_{(0.5-2.0\text{keV})} \sim 10^{41}$ and $\sim 10^{39}$ erg s $^{-1}$ respectively). These objects in fact appear similar to MS 0317.7–6647, the brightest unidentified object of the EMSS (Stoeckle et al. 1995), and to the ultraluminous X-ray sources which are now being found by *Chandra* (e.g. Fabbiano, Zezas & Murray 2001; Blanton, Sarazin & Irwin, 2001; Sarazin, Irwin & Bregman, 2000; 2001; Cagnoni et al. 2002).

7.6. Unknown nature

1WGA J1220.6+3347

1WGA J1220.6+3347 was detected by the *Einstein* IPC as an ultra-soft source (Thompson, Shelton & Arning 1998) with $CR = 0.012 \pm 0.002$ counts s $^{-1}$ more than 10 years before the PSPC observation. *Einstein* CR is consistent within the errors with the predictions based on the PSPC CR. The *Einstein* and Galpipe PSPC positions are $22''$ apart and so are consistent.

1WGA J1233.3+6910

This source is listed in Radecke (1997) with a position of 12:33:23.69 +69:10:05.5 and a count rate of 0.0225 counts

¹⁰In 1993 the source is detected in the outer rim and spread over a large area and a variability study is not possible due to the low signal to noise. The count rate, however, is consistent with that of the 1991 observation

s^{-1} . For the same observation we found a position $20.4''$ away (Table 1) and a count rate of $0.0214 \pm 0.0013 \text{ counts s}^{-1}$. 5 years after the PSPC observation, the source was detected by the HRI; however the source falls on the detector edge, making any flux and positional estimate unreliable.

1WGA J1420.0+0625

1WGA J1420.0+0625 was observed twice by *ROSAT* and is consistent with no variability within each observation and on a 6-month timescale.

7.6.1. Discussion on the unknown sources

The three sources presented above, besides being all persistent, have similar unexceptional X-ray spectral shapes ($\Gamma \sim 2.2 - 2.4$), $N_H = N_{H(\text{Gal.})}$ (Table 3), lack a red Palomar counterpart and have $f_X/f_V \geq 15$ (Table 4). Could we be seeing the reflected component of an intrinsically bright obscured AGN?

8. COMPARISON WITH PREVIOUS SURVEYS

A number of different projects to identify X-ray-discovered sources have been carried out over the last decade. Although the major goal of these studies was not to search for blanks, they were nevertheless discovered as a few percent ‘remnant’ of unidentified sources (e.g. Bade et al. 1995; Schwöpe et al. 2000, and references therein). For instance, Schwöpe et al. (2000 and references therein) presented a large sample of optically (un)identified *ROSAT* sources, in which there were three cases of blanks¹¹. Blanks usually constitute $\sim 5 - 8\%$ of all wide-angle surveys, regardless of survey depth. Because their optical faintness prevents easy investigation, blanks have not been investigated further in these general purpose wide-angle surveys.

Blanks are also found in deep fields (e.g. CDFN, Alexander et al. 2001; UDS, Lehmann et al. 2000), and these are usually investigated in greater detail than in wide-angle surveys, despite being even more difficult to follow-up, because of the great interest in deep survey identifications in general.

Wide-angle surveys might be expected to trace different populations than narrow-angle deep fields. Yet a comparison of our identifications with those of the CDFN, UDS and UK-RDS shows that they overlap quite strongly. The counterparts of blanks found in these deep fields are usually red. The favored classifications are high redshift obscured quasars, and high redshift ($z \sim 1$) clusters of galaxies (e.g. Newsam et al. 1997; Alexander et al. 2001; Lehmann et al. 2001). This makes the bright blanks from our, and other, wide-field surveys of immediate interest for understanding the faint source population. Being 100-1000 times brighter in X-rays, they are far easier to study in detail. As a result we anticipate that they will become intensely studied.

9. SUMMARY AND CONCLUSIONS

We have identified a population of blank field sources among the *ROSAT* bright X-ray sources with faint optical counterparts, i.e. $O > 21.5$ on the Palomar Sky survey. Their extreme X-ray over optical flux ratio ($f_X/f_V > 10$) is not compatible with the main classes of X-ray emitters, except for BL Lacs for the less extreme cases. The identification process brought to the discovery of two high z , high luminosity clusters of galaxies (§ 7.4.1), one BL Lacertae object (§ 7.1), and two type 1 AGNs (§ 7.3.1). Four blanks are AGN-like sources (§ 7.3.1) which

seem to form a well defined group: they present type 1 X-ray spectra and red Palomar counterparts. These sources are similar to the galaxies with bright X-ray emission ($L_X \sim 10^{42} - 10^{43} \text{ erg s}^{-1}$) but weak or absent AGN features in the optical band found since *Einstein* observations (Elvis et al. 1981; Tananbaum et al. 1997) and which are now being found in large numbers (e.g. Della Ceca et al. 2001; Hornschemeier et al. 2001, Fiore et al. 2001). We considered possible explanations for the discrepancy between X-ray and optical data: a suppressed BBB emission; an extreme dust to gas ratio; a dust grain size distribution different from the Galactic one; a dusty warm absorber and an high redshift ($z \geq 3.5$) QSO nature. Two sources (§ 7.5) are candidate ultraluminous X-ray binaries within nearby galaxies (see also Cagnoni et al. 2002). Three sources (§ 7.6) have a still unknown nature; for each of them we listed and justified the possibilities excluded.

To make progress in understanding the nature of blanks we need to identify them with optical or near infrared counterparts. Since both in the case of obscured AGNs and of high redshift clusters of galaxies red counterparts are expected, we obtained optical (R band) and infrared (K band) imaging for the 16 fields in our sample at a 4m-class telescope and we will present the results in a future paper.

The obvious next step is to construct a larger and statistically complete sample of blank field sources. For this purpose, the *XMM-Newton* and *Chandra* catalogs soon available will form a good basis. The smaller positional uncertainty will cut down on false optical identifications and so will considerably *increase* the percentage of blanks found ($\sim 14\%$ at $f_X \geq 10^{-13} \text{ erg cm}^{-2} \text{ s}^{-1}$, Maccacaro & Della Ceca private communication). The smaller PSF of these new detectors will also allow the direct separation of extended sources, enabling high redshift clusters of galaxies to be found even more readily.

This work made use of: the NASA/IPAC Extragalactic Database (NED) which is operated by the Jet Propulsion Laboratory, California Institute of Technology, under contract with the National Aeronautics and Space Administration; the HEASARC archive, a service of the Laboratory for High Energy Astrophysics (LHEA) at NASA/ GSFC and the High Energy Astrophysics Division of the Smithsonian Astrophysical Observatory (SAO); the SIMBAD database, operated at CDS, Strasbourg, France.

I.C. thanks Fabrizio Fiore for making his program to compute the effective spectral indices available, Alessandro Caccianiga for the electronic format of his data used for Figure 5 and Roberto Della Ceca, Paola Severgnini and Aldo Treves for useful scientific discussions. We thank the anonymous referee for the carefull and deep work and for helpful comments and suggestions, which improved the quality of this paper. This work was supported by NASA ADP grant NAG5-9206 and by the Italian MIUR (IC and AC). I.C. acknowledges a CNAA fellowship.

¹¹These 3 blanks are not included in our sample because they were detected only with the HRI, or with the PSPC data after the release of WGACAT95.

REFERENCES

- Bade, N., Fink, H. H., Engels, D., Voges, W., Hagen, H.-J., Wisotzki, L. & Reimers, D., 1995, A&AS, 110, 469
- Bade, N., Komossa, S., & Dahlem, M. 1996, A&A, 309, L35
- Blanton, E. L., Sarazin, C. L., & Irwin, J. A. 2001, ApJ, 552, 106
- Becker, R. H., White, R. L. & Helfand, D. J., 1995, ApJ, 450, 559
- Block, D. L., Witt, A. N., Grosbøl, P., Stockton, A., & Moneti, A. 1994, A&A, 288, 383
- Borgani, S. & Guzzo, L., 2001, Nature, 409, 39
- Borgani, S. et al., 2001, ApJ, 2001, 561, 13
- Boyle, B. J., McMahon, R.G., Wilkes, B. J. & Elvis, M., 1995, MNRAS, 272, 462
- Boyle, B. J., Wilkes, B. J. & Elvis, M., 1997, MNRAS, 285, 511
- Brandt, W. N., Fabian, A. C., & Pounds, K. A. 1996, MNRAS, 278, 326
- Caccianiga, A., Maccacaro, T., Wolter, A., Della Ceca, R. & Gioia, I. M., 1999, ApJ, 513, 51
- Cagnoni, I., Elvis, M., Kim, D.-W., Mazzotta, P., Huang, J.-S. & Celotti, A., 2001a, ApJ, 560, 86
- Cagnoni, I., Elvis, M., Kim, D.-W., Mazzotta, P., Huang, J.-S. & Celotti, A., 2001b, in press, (astro-ph/0105430) Proceeding of the conference "Clusters and the High-Redshift Universe observed in X-rays" March 10-17, 2001, Les Arcs, Savoie, France
- Cagnoni, I., Turolla, R., Treves, A., Huang, J.-S., Kim, D. W., Elvis, M. & Celotti, A., 2002, ApJ, submitted
- Carkner, L., Feigelson, E. D., Koyama, K., Montmerle, T., Reid, I. N., 1996, ApJ, 464, 286
- Colbert, E. & Ptak, A., 2002, ApJS submitted (astro-ph/0204002)
- Coleman, G. D., Wu, C.-C. & Weedman, D. W., 1980, ApJS, 43, 393
- Colpi, M., Turolla, R., Zane, S. & Treves, A., 1998, ApJ, 501, 252
- Comastri, A., Fiore, F., Vignali, C., Matt, G., Perola, G.C. & La Franca, F., 2001, MNRAS, 327, 781
- Comastri, A. et al. 2002, in press (astro-ph/0203019)
- Condon, J. J., Cotton, W. D., Greisen, E. W., Yin, Q. F., Perley, R. A., Taylor, G. B. & Broderick, J. J., 1998, AJ, 115, 1693
- Costamante, L., et al., 2001, A&A, 371, 521
- Della Ceca, R., Scaramella, R., Gioia, I. M., Rosati, P., Fiore, F. & Squires, G., 2000, A&A, 353, 498
- Di Matteo, T., Quataert, E., Allen, S. W., Narayan, R. & Fabian, A. C., 2000, MNRAS, 311, 507
- Ebeling, H. et al. 2000, ApJ, 534, 133
- Ebeling, H., Jones, L. R., Fairley, B. W., Perlman, E., Scharf, C., & Horner, D. 2001, ApJ, 548, L23
- Elvis, M., Schreier, E. J., Tonry, J., Davis, M. & Huchra, J. P., 1981, ApJ, 246, 20
- Elvis, M., Risaliti, G. & Zamorani, G., 2002, ApJL in press, (astro-ph/0112413)
- Fabbiano, G. 1989, ARA&A, 27, 87
- Fabbiano, G., Zezas, A., & Murray, S. S. 2001, ApJ, 554, 1035
- Fabian, A.C. & Iwasawa, K., 1999, MNRAS, 303, L34
- Fiore, F., Elvis, M., Giommi, P. & Padovani, P., 1998, ApJ, 492, 79
- Fossati, G., Maraschi, L., Celotti, A., Comastri, A. & Ghisellini, G., 1998, MNRAS, 299, 433
- Francis, P. J., Hewett, P. C., Foltz, C. B., Chaffee, F. H., Weymann, R. J. & Morris, S. L., 1991, ApJ, 373, 465
- Frontera, F. et al., 2000, ApJS, 127, 59
- Gardner, J.P., Cowie L.L. & Wainscoat R.J., 1993, ApJ, 415, L9
- George, I. M. et al., 2000, ApJ, 531, 52
- Gilli, R., Salvati, M. & Hasinger, G., 2001, A&A, 366, 407
- Gioia, I. M. & Luppino, G. A., 1994, ApJS, 94, 538
- Greiner, J., Hartmann, D. H., Voges, W., Boller, T., Schwarz, R. & Zharikov, S. V. 2000, A&A, 353, 998
- Haberl, F., Motch, C., Buckley, D.A.H., Zickgraf, F. & Pietsch, W., 1997, A&A, 326, 662
- Haberl, F., Motch, C. & Pietsch, W., 1998, Astron. Nachr., 319, 97
- Haberl, F., Pietsch, W. & Motch, C., 1999, A&A, 351, L53
- Halpern, J. P., Turner, T. J. & George, I. M., 1999, MNRAS, 307, 47
- Hartmann D.H. & MacFadyen A.I., 1999, Proc. 19th Texas Symp. on Relativistic Astrophysics & Cosmology, Paris, Dec. 1998
- Henry, J. P., 2000, ApJ, 534, 565
- Hornschemeier, A. E., et al., 2001, ApJ, 554, 742
- Huang, J.-S., et al. 2001, A&A, 368, 787
- Janka, H.-T. & Ruffert, M., 1996, A&A, 307, L33
- Kim, D.-W. & Elvis, M., 1999, ApJ, 516, 9
- Komossa, S. & Fink, H. 1997, A&A, 327, 555
- Komossa, S. & Bade, N. 1998, A&A, 331, L49
- Koyama, K., et al., 1994, PASJ, 46, L125
- Lamer, G., Brunner, H. & Staubert, R., 1997, A&A, 37, 467
- Laor, A., Fiore, F., Elvis, M., Wilkes, B. J., & McDowell, J. C. 1997, ApJ, 477, 93
- Leighly, K. M. 1999, ApJS, 125, 297
- Livio, M., Xu, C. & Frank, J., 1998, ApJ, 492, 298
- Maccacaro, T., Perola, G.C. & Elvis, M., 1982, ApJ, 257, 47
- Maccacaro, T., Gioia, I. M., Wolter, A., Zamorani, G. & Stocke, J. T., 1988, ApJ, 326, 680
- Madau, P. & Blaes, O., 1994, ApJ, 423, 748
- Maiolino, R., Marconi, A. & Oliva, E., 2001a, A&A, 365, 37
- Maiolino, R., et al. 2001b, A&A, 365, 28
- Makishima, K. et al. 2000, ApJ, 535, 632
- Maoz, E., Ofek, E.O. & Shemi, A., 1997, MNRAS, 287, 293
- Maraschi, L., Fossati, G., Tagliaferri, G. & Treves, A., 1995, ApJ, 443, 578
- Mason, K. O., et al. 2000, MNRAS, 311, 456
- McMahon, R.G. & Irwin, M.J., 1992, in Digitized Optical Sky Surveys, ed. H.T. MacGillivray & E.B. Thomson (Dordrecht: Kluwer), 417
- Moles, M., Garcia-Pelayo, J. M., Masegosa, J. & Aparicio, A., 1985, ApJS, 58, 255
- Motch, C., Harbel, F., Zickgraf, F., Hasinger, G. & Schwobe, A.D., 1999, A&A, 351, 177
- Narayan, R. & Yi, I., 1994, ApJ, 428, L13
- Narayan, R., Mahadevan, R., Grindlay, J. E., Popham, R. G. & Gammie, C., 1998, ApJ, 492, 554
- Nicastro, F., Fiore, F. & Matt, G., 1999, ApJ, 517, 108
- Pian, E., et al., 1998, ApJ, 492, L17
- Popov, S., Colpi, M., Treves, A., Turolla, R., Lipunov, V. M. & Prokhorov, M. E., 2000, ApJ, 530, 896
- Popov, S., Colpi, M., Treves, A. & Turolla, R., 2002, proceedings of the conference ICGA-V in Gravitation & Cosmology (2002)
- Prandoni, I., et al., 1999, A&A, 345, 448
- Press, W.H. & schecter, P., 1974, ApJ, 187, 425
- Puchnarewicz, E. M., Mason, K. O., Siemiginowska, A. & Pounds, K. A., 1995, MNRAS, 276, 20
- Puchnarewicz, E. M., Mason, K. O., Siemiginowska, A., Fruscione, A., Comastri, A., Fiore, F. & Cagnoni, I., 2001, ApJ, 550, 644
- Radecke, H.-D., 1997, A&A, 319, 18
- Raymond, J. C. & Smith, B. W., 1977, ApJS, 35, 419
- Risaliti, G., Marconi, A., Maiolino, R., Salvati, M. & Severgnini, P., 2001, A&A, 371, 37
- Roberts, T. P. & Warwick, R. S., 2000, MNRAS, 315, 98
- Romer, A. K., et al., 2000, ApJS, 126, 209
- Rosati, P., della Ceca, R., Norman, C. & Giacconi, R., 1998, ApJ, 492, L21
- Rosati, P., Stanford, S. A., Eisenhardt, P. R. Elston, R., Spinrad, H., Stern, D. & Dey, A., 1999, AJ, 118, 76
- Sarazin, C. L., Irwin, J. A., & Bregman, J. N. 2001, ApJ, 556, 533
- Sarazin, C. L., Irwin, J. A., & Bregman, J. N. 2000, ApJ, 544, L101
- Schmidt, M., et al., 1998, A&A, 329, 495
- Schwobe, A.D., Hasinger, G., Schwarz, R., Haberl, F. & Schmidt, M., 1999, A&A, 341, L51
- Shakura, N. I. & Sunyaev, R. A., 1973, A&A, 24, 337
- Stanford, S. A., Holden, B., Rosati, P., Tozzi, P., Borgani, S., Eisenhardt, P. R. & Spinrad, H., 2001, ApJ, 552, 504
- Stark, A. A., Gammie, C. F., Wilson, R. W., Bally, J., Linke, R. A., Heiles, C. & Hurwitz, M., 1992, ApJS, 79, 77
- Stocke, J. T., Wang, Q.D., Perlman, E.S., Donahue, M.E. & Schachter, J.F., 1995, AJ, 109, 1199
- Tananbaum, H., Tucker, W., Prestwich, A. & Remillard, R., 1997, ApJ, 476, 83
- Thompson, R. J., Shelton, R. G. & Arning, C. A., 1998, AJ, 115, 258
- Tozzi, P. & Norman, C., 2001, ApJ, 546, 63
- Treves, A., Turolla, R., Zane, S. & Colpi, M., 2000, PASP, 112, 297
- Tucker, W.H., Tananbaum, H. & Remillard, R.A., 1995, ApJ, 444, 532
- Turner, T. J., George, I. M., Nandra, K., & Turcan, D. 1999, ApJ, 524, 667
- Ueda, Y., Ishisaki, Y., Takahashi, T., Makishima, K., and Ohashi, T., 2001, ApJS, 133, 1
- Urry, C. M. & Padovani, P., 1995, PASP, 107, 803
- Urry, C. M., Sambruna, R. M., Worrall, D. M., Kollgaard, R. I., Feigelson, E. D., Perlman, E. S. & Stocke, J. T., 1996, ApJ, 463, 424
- Voges, W., et al., 1999, A&A, 349, 389
- Vogler, A., Pietsch, W. & Kahabka, P., 1996, A&A, 305, 74
- Walter, F. M., Wolk, S. J. & Neuhauser, R., 1996, Nature, 379, 233
- Walter, F. M., 2001, ApJ, 549, 433
- White, N., Giommi, P. & Angelini, L., 1995, WGACAT, <http://heasarc.gsfc.nasa.gov/W3Browse/all/wgacat.html>
- White, S.D.M. & Frenk, C.S., 1991, ApJ, 379, 52
- Wichmann, R. et al., 1996, A&A, 312, 439
- Whittet, D. C. B. 1992, Dust in the galactic environment, Institute of Physics Publishing, 306 p.,
- Zampieri, L., Turolla, R., Zane, S. & Treves, A., 1995, ApJ, 439, 849
- Zampieri, L., Campana, S., Turolla, R., Chierigato, M., Falomo, R., Fugazza, D., Moretti, A. & Treves, A., 2001, A&A, 378, L5
- Zezas, A., Fabbiano, G., Rots, A. H. & Murray, S. S., 2002, ApJS submitted (astro-ph/0203174)
- Zombeck, M. V. 1990, Cambridge: University Press, 1990, 2nd ed.,

TABLE 1
THE FINAL SAMPLE OF 16 SOURCES.

Source name (1WGA J)	Best coords ^a Ra, Dec (J2000)	PSPC count rate ^b	HRI count rate ^c	POSS E	POSS O	POSS O-E ^d	F_X/F_V
0221.1+1958	02 21 09.0, 19 58 15.3	1.29 ± 0.09	—	-	-	-	>21.3
0432.4+1723	04 32 29.6, 17 23 47.8	1.42 ± 0.10	—	20.0	-	> 1.5	>38.5
0951.4+3916	09 51 28.7, 39 16 36.8	0.90 ± 0.10	—	19.1	-	> 2.4	>13.0
1103.5+2459	11 03 35.4, 24 59 09.6	0.33 ± 0.04	—	18.2	-	> 3.3	>3.5
1216.9+3743	12 16 57.1, 37 43 35.4	1.26 ± 0.15	< 0.23 ^f	-	-	-	>13.5
1220.3+0641	12 20 18.3, 06 41 25.7 ^e	4.42 ± 0.39	2.94 ± 0.53	18.58	21.81	3.23	102.1
1220.6+3347	12 20 38.4, 33 47 26.7	0.65 ± 0.07	—	20.9	21.7	0.8	14.6
1226.9+3332	12 26 57.6, 33 33 00.9 ^e	2.00 ± 0.12	0.87 ± 0.15	-	-	-	>41.4
1233.3+6910	12 33 25.5, 69 10 14.6	2.14 ± 0.13	on the border	-	-	-	>38.4
1243.6+3204	12 43 41.1, 32 04 56.6 ^e	0.67 ± 0.08	0.34 ± 0.06	-	-	-	>9.7
1340.1+2743	13 40 10.3, 27 43 38.9	4.74 ± 0.23	—	-	-	-	>83.4
1412.3+4355	14 12 21.4, 43 55 01.0 ^e	0.53 ± 0.06	0.19 ± 0.09	18.73	-	> 2.77	>9.0
1415.2+4403	14 15 15.0, 44 03 20.2	0.30 ± 0.06	—	-	-	-	>6.0
1416.2+1136	14 16 13.2, 11 36 17.9 ^e	0.31 ± 0.08	0.21 ± 0.09	19.5	22.22	2.72	10.7
1420.0+0625	14 20 05.6, 06 25 25.0	0.85 ± 0.09	—	-	-	-	>15.7
1535.0+2336	15 35 06.1, 23 37 03.2 ^e	0.37 ± 0.07	0.14 ± 0.03	19.6	21.8	2.2	10.2

^aBest X-ray coordinates: Galpipe ($\pm 13''$ 1σ) or HRI ($\pm 1\sigma$) when available.

^bbetween 0.5 and 2.0 keV in units of 10^{-2} counts s^{-1} .

^c 10^{-2} counts s^{-1} .

^dAssuming O magnitude equal to V magnitude and O>21.5 when no source is detected in the Palomar O band

^eHRI coordinates

^f 3σ upper limit in a $r = 24''$ circle

TABLE 2
ALL AVAILABLE *ROSAT* OBSERVATIONS FOR THE 16 BLANK FIELD SOURCES.

(1WGA J)	ROR	PSPC observations			ROR	HRI observations	
		Date	Exposure	Counts ^a		Date	Exposure
0221.1+1958	900147n00 ^c	07-30-1991	24947	365	–	–	–
0432.4+1723	200443n00 ^c	03-07-1991	20074	313	–	–	–
	201313n00	09-10-1992	4027	–	–	–	–
	900353n00	02-21-1993	7718	–	–	–	–
0951.4+3916	701367n00	10-26-1993	14281	116	–	–	–
1103.5+2459	300291n00 ^c	05-26-1993	44010	357	–	–	–
1216.9+3743	600179n00	11-21-1991	9304	135	702724n00	06-20-1996	8752
1220.3+0641	700021n00 ^c	12-20-1991	3430	337	702172n00	12-10-1995	2348
	–	–	–	–	702173n00	12-11-1996	2662
	–	–	–	–	702174n00	12-12-1995	3183
	–	–	–	–	702188n00	06-07-1996	3951
	–	–	–	–	702189n00	07-06-1996	3835
	–	–	–	–	702210n00	12-09-1995	2476
	–	–	–	–	702211n00	12-17-1995	3839
	–	–	–	–	702212n00	12-23-1995	890
1220.6+3347	700864n00	06-20-1992	3009	427 ^b	–	–	–
	700864a01	05-23-1993	19284	427 ^b	–	–	–
1226.9+3332	600173n00	06-02-1992	8002	538 ^b	702725n00	06-23-1996	11353
	600277n00	06-17-1992	9036	538 ^b	–	–	–
1233.3+6910	300034n00	04-04-1991	15040	671	300492n00	10-08-1996	41834
1243.6+3204	600416n00 ^c	06-28-1992	18052	103	600605n00	05-29-1994	27669
1340.1+2743	300333n00	07-06-1993	13083	2220 ^b	–	–	–
	300333a01	07-02-1994	14599	2220 ^b	–	–	–
	701063n00	07-15-1992	10032	2220 ^b	–	–	–
	701065n00	07-11-1992	8971	2220 ^b	–	–	–
	701067n00	07-14-1992	8209	2220 ^b	–	–	–
	701069n00 ^c	07-13-1992	9912	822	–	–	–
	701459n00	07-06-1993	7157	2220 ^b	–	–	–
1412.3+4355	700248n00	06-26-1991	24843	306	–	–	–
1415.2+4403	700248n00	06-26-1991	24843	322	–	–	–
1416.2+1136	700122n00	07-20-1991	27863	265	701858n00	07-16-1995	11345
1420.0+0625	700865n00	07-25-1992	10710	268 ^b	–	–	–
	700865a01	01-12-1993	8876	268 ^b	–	–	–
1535.0+2336	701411n00 ^c	07-24-1993	22955	130	701330n00	07-29-1994	35661

^aSource net counts in each observation between 0.07 and 2.4 keV

^bCalculated in the combined image of all the available PSPC observations

^cWGA observation

TABLE 3
SPECTRAL FITS WITH: AN ABSORBED POWER LAW, A BLACK BODY AND AN ABSORBED RAYMOND-SMITH MODEL

Source name 1WGA J	Absorbed power law					Absorbed Black body				Absorbed Raymond-Smith			
	Γ^a	k^b	N_H^c	$N_{H(gal)}^d$	χ_r^{2e}	kT^f	k^b	N_H^c	χ_r^{2e}	kT^g	z	k^b	χ_r^{2e}
0221.1+1958	$2.33^{+0.65}_{-0.47}$	$0.96^{+0.34}_{-0.16}$	$12.29^{+9.03}_{-5.23}$	9.59	0.96	303^{+38}_{-15}	$2.23^{+0.25}_{-0.19}$	$2.62^{+4.19}_{-1.91}$	1.16	$2.23^{+1.21}_{-0.57}$	$0.49^h_{-0.38}$	$7.91^{+16.76}_{-7.91}$	0.96
0432.4+1723	2.15 ± 0.28	$9.21^{+0.37}_{-1.00}$	fixed	—	0.93	496^{+108}_{-82}	$3.88^{+1.14}_{-0.60}$	$2.72^{+6.83}_{-2.35}$	0.84	$0.32^{+0.09}_{-0.05}$	$1.98^h_{-0.77}$	$942^{+26.29}_{-7.26}$	1.29
	$1.03^{+0.68}_{-0.46}$	$0.92^{+0.44}_{-0.17}$	$9.42^{+12.40}_{-5.34}$	13.1	0.77								
0951.4+3916	$1.20^{+0.23}_{-0.26}$	$10.56^{+6.29}_{-1.33}$	fixed	—	0.95	295^{+65}_{-60}	$1.71^{+0.93}_{-0.29}$	$7.40^{+16.26}_{-5.85}$	0.94	$64.00^h_{-52.68}$	0.01^h_h	$2.93^{+9.42}_{-2.93}$	1.40
	$2.62^{+2.14}_{-0.81}$	$0.82^{+1.72}_{-1.64}$	$20.19^{+3.99}_{-1.09}$	1.55	0.93								
1103.5+2459	$0.92^{+0.25}_{-0.28}$	$4.21^{+0.39}_{-0.67}$	fixed	—	1.29	222^{+64}_{-49}	$0.55^{+0.09}_{-0.07}$	$0.0^{+0.15}_h$	1.69	$2.84^{+1.49}_{-0.93}$	$2.00^h_{-1.22}$	$6.72^{+0.77}_{-6.72}$	1.17
	1.67 ± 0.31	0.16 ± 0.02	$0.35^{+0.82}_{-0.29}$	1.38	0.92								
1216.9+3743	$2.10^{+0.17}_{-0.18}$	$1.76^{+0.20}_{-0.25}$	fixed	—	0.94	194^{+82}_{-77}	$3.41^{+54.51}_{-3.41}$	$14.94^{+48.54}_{-12.62}$	0.82	$0.77^{+0.13}_{-0.10}$	$0.00^{+0.04}_h$	$1.18^{+0.42}_{-0.33}$	0.96
	$4.90^{+5.10}_{-1.74}$	$2.17^{+4.35}_{-19.43}$	$44.78^{+8.72}_{-2.43}$	1.69	0.81								
1220.3+0641	$1.34^{+0.25}_{-0.31}$	$5.76^{+0.40}_{-1.27}$	fixed	—	1.16	174	7.99	3.93×10^{-8}	2.67	$2.52^{+0.62}_{-0.42}$	$2.00^h_{-0.68}$	$97.3^{+3.3}_{-97.3}$	1.67
	$1.95^{+0.28}_{-0.25}$	$2.22^{+0.27}_{-0.17}$	$1.28^{+0.66}_{-0.54}$	1.56	1.34								
1220.6+3347	2.07 ± 0.10	$23.39^{+1.67}_{-2.66}$	fixed	—	1.29	147^{+8}_{-7}	1.52 ± 0.12	$0.0^{+0.10}_h$	1.63	$1.77^{+0.35}_{-0.47}$	$2.00^h_{-0.69}$	$20.8^{+2.4}_{-20.8}$	1.88
	2.31 ± 0.33	$0.37^{+0.03}_{-0.06}$	$1.40^{+0.29}_{-0.68}$	1.27	0.63								
1226.9+3332	2.26 ± 0.11	$3.70^{+0.29}_{-0.59}$	fixed	—	0.60	300^{+30}_{-26}	$3.37^{+0.24}_{-0.22}$	$0.0^{+0.09}_h$	1.93	$7.42^{+9.18}_{-2.81}$	0.56^h_h	$8.89^{+16.97}_{-8.89}$	1.07
	$1.51^{+0.24}_{-0.23}$	$1.06^{+0.12}_{-0.05}$	$1.66^{+0.84}_{-0.64}$	1.38	1.08								
1233.3+6910	1.42 ± 0.11	$11.05^{+0.40}_{-0.98}$	fixed	—	1.04	187	4.04	1.12×10^{-10}	2.5	$2.23^{+0.53}_{-0.50}$	$1.75^h_{-0.45}$	$43.4^{+8.7}_{-43.4}$	1.47
	$2.43^{+0.20}_{-0.18}$	$1.17^{+0.07}_{-0.09}$	$2.60^{+0.57}_{-0.53}$	1.69	1.39								
1243.6+3204	2.12 ± 0.08	$11.39^{+0.50}_{-1.03}$	fixed	—	1.45	770^{+40}_{-58}	$11.33^{+210.38}_{-11.33}$	$110.5^{+109.5}_{-49.0}$	0.48	$64.0^h_{-30.76}$	$0.0^{+0.89}_h$	$2.26^{+2.65}_{-2.26}$	1.76
	$5.97^{+6.62}_{-2.59}$	$18.3^{+366.7}_{-36.7}$	$171.3^{+149.5}_{-78.3}$	1.23	0.49								
1340.1+2743	$0.07^{+0.22}_{-0.53}$	$3.14^{+0.35}_{-0.61}$	fixed	—	0.84	213	8.35	4.04×10^{-6}	2.15	2.69	0.46	20.0	2.04
	2.35 ± 0.18	$1.18^{+0.09}_{-0.04}$	$2.99^{+0.58}_{-0.54}$	1.09	0.53								
1412.3+4355	1.72 ± 0.06	$10.83^{+0.42}_{-0.55}$	fixed	—	1.25	168^{+21}_{-16}	0.93 ± 0.11	$0.0^{+0.12}_h$	0.77	$2.57^{+1.25}_{-0.60}$	$1.96^h_{-1.16}$	$9.68^{+1.29}_{-9.68}$	0.50
	$1.76^{+0.30}_{-0.30}$	0.25 ± 0.03	$0.06^{+0.09}_{-0.03}$	1.16	0.48								
1415.2+4403	2.02 ± 0.16	$0.26^{+0.02}_{-0.43}$	fixed	—	0.48	123^{+10}_{-12}	$0.98^{+0.79}_{-0.17}$	$(1.05^{+3594}_h) \times 10^{-4}$	1.57	$1.04^{+0.24}_{-0.14}$	$1.91^h_{-0.37}$	$16.5^{+2.7}_{-16.5}$	1.31
	$2.97^{+0.50}_{-0.43}$	$0.146^{+0.03}_{-0.04}$	$1.72^{+0.96}_{-0.72}$	1.17	1.13								
1416.2+1136	$2.70^{+0.22}_{-0.20}$	$1.52^{+0.25}_{-0.48}$	fixed	—	1.12	145 ± 14	$0.79^{+0.23}_{-0.14}$	$0.0^{+0.64}_h$	0.95	$1.23^{+0.33}_{-0.52}$	$1.94^h_{-0.96}$	$15.4^{+2.83}_{-15.4}$	0.89
	$2.98^{+1.11}_{-0.69}$	$0.14^{+0.06}_{-0.03}$	$2.61^{+3.11}_{-1.78}$	1.81	0.90								
1420.0+0625	$2.68^{+0.27}_{-0.24}$	$1.54^{+0.31}_{-0.54}$	fixed	—	0.86	259^{+33}_{-27}	1.42 ± 0.15	$0.0^{+0.4}_h$	0.88	$2.92^{+5.09}_{-1.69}$	1.03^h_h	$7.31^{+6.17}_{-7.31}$	0.80
	$2.21^{+0.38}_{-0.34}$	$0.52^{+0.06}_{-0.08}$	$3.84^{+2.23}_{-1.58}$	2.18	0.82								
1535.0+2336	$1.79^{+0.17}_{-0.19}$	$4.66^{+0.46}_{-0.51}$	fixed	—	0.82	1150^h_h	3.16^h_h	$0.0^{+20.58}_h$	1.74	$64^h_{-61.22}$	0.00^h_h	$1.16^{+4.33}_{-1.16}$	1.76
	$0.70^{+0.72}_{-1.05}$	$0.14^{+0.04}_{-0.04}$	$0.16^{+2.37}_{-0.16}$	4.26	1.67								
absorbed sample	$0.47^{+1.72}_{-1.68}$	1.40 ± 0.66	fixed	—	1.66	372^{+86}_{-75}	$1.99^{+0.35}_{-0.22}$	$6.53^{+7.73}_{-5.07}$	0.49	$64.0^h_{-34.63}$	$0.00^{+1.09}_h$	$2.28^{+3.35}_{-2.28}$	0.96
	$2.03^{+1.21}_{-1.02}$	$0.90^{+0.76}_{-0.90}$	$23.31^{+20.58}_{-15.33}$	1.49	0.46								
unabsorbed sample	$0.48^{+0.21}_{-0.24}$	$0.46^{+0.30}_{-0.38}$	(1.49)fixed	—	0.72	208	— ⁱ	0.	2.54	$3.49^{+0.63}_{-0.53}$	$1.79^h_{-0.44}$	— ⁱ	1.41
	1.85 ± 0.1	— ⁱ	$1.43^{+0.28}_{-0.15}$	1.45	1.27								
	1.86 ± 0.04	— ⁱ	1.45(fixed)	—	1.26								

^aPhoton index

^bnormalizations at 1 keV in 10^{-4} for the power law and the Raymond-Smith models and in 10^{-6} ph cm⁻² s⁻¹ keV⁻¹ for the blackbody model

^cHydrogen column density for an absorbed power law in 10^{20} atoms cm⁻²

TABLE 4
X-RAY (ABSORBED) FLUXES FOR THE 16 BLANK FIELD SOURCES.

Source name (1WGA J)	Class.	F_X^a (0.3-3.5 keV)	F_X^a (0.5-2.0 keV)	F_X^a (0.05-2.5 keV)	F_{WGA}^b (0.05-2.5 keV)	F_X/F_{WGA} (0.05-2.5 keV)	F_X/F_V^c
0221.1+1958	High N_{HGal} .	2.28	1.47	1.91	1.98	0.96	>21.3
0432.4+1723	High N_{HGal} .	4.12	1.80	2.63	1.69	1.56	>38.5
0951.4+3916	Absorbed	1.39	0.99	1.19	2.59	0.46	>13.0
1103.5+2459 ^d	Unabsorbed	0.64	0.37	0.64	1.01	0.63	>3.4
1216.9+3743	Absorbed	1.45	1.22	1.40	2.80	0.50	>13.5
1220.3+0641	Unabsorbed	8.22	4.74	7.90	14.39	0.53	102.6
1220.6+3347	Unabsorbed	1.30	0.79	1.40	2.00	0.70	14.6
1226.9+3332	Unabsorbed	4.44	2.43	3.61	3.61	1.00	>41.4
1233.3+6910	Unabsorbed	4.11	2.41	4.15	2.99	1.39	>38.4
1243.6+3204	Absorbed	1.04	0.83	0.96	1.28	0.75	>9.7
1340.1+2743	Unabsorbed	8.94	5.60	8.70	10.14	0.86	>83.4
1412.3+4355 ^d	Unabsorbed	0.97	0.56	0.97	1.63	0.60	>9.0
1415.2+4403	Unabsorbed	0.64	0.32	0.81	1.21	0.67	>6.0
1416.2+1136	Unabsorbed	0.59	0.30	0.69	1.11	0.62	10.7
1420.0+0625	Unabsorbed	1.68	1.05	1.53	2.80	0.53	>15.7
1535.0+2336	High N_{HGal} .	0.83	0.36	0.55	1.04	0.53	10.2

^ain units of 10^{-13} erg cm⁻² s⁻¹ and computed assuming the best fit absorbed power law model with free absorption.

^bin units of 10^{-13} erg cm⁻² s⁻¹ and computed using a constant correction factor of 1.5×10^{-11} erg cm⁻² s⁻¹.

^c F_X in the 0.3-3.5 keV band divided by F_V

^dSince the fit with an absorbed power law model with free absorption gives a ~ 4 times lower than Galactic absorbing column, we froze the absorption to the Galactic value.

TABLE 5
SOURCES DETECTED IN THE RASS

Source name (1WGA J)	Offset ^a (")	RASS count rate ^b	Pointed Obs. count rate ^c	RASS Obs. Date	Pointed Obs. Obs. Date
1220.3+0641	10.5	8 ± 2	9.88 ± 0.64	not available	12-1991
1220.6+3347	13.9	3.12 ± 1.06	1.92 ± 0.14	12-1990	06-1992 and 5-1993
1233.3+6910	15.6	2.77 ± 0.83	4.48 ± 0.24	11-1990	04-1991

^aOffset calculated from the positions in Table 1

^bIn units of 10^{-2} counts s^{-1} .

^cFull band PSPC count rate in units of 10^{-2} counts s^{-1} .

TABLE 6
ASCA SERENDIPITOUS OBSERVATIONS OF ROSAT BLANK FIELD SOURCES.

Source name (1WGA J)	ROR	Date	Exposure (ks) ^b	Count Rate ^a
1220.3+0641	74074000	12-25-1995	46	21.4 ^c
1226.9+3332	76006000	05-24-1998	44	3.83 ± 0.48 ^d
	78009000	05-25-2000	77	^e
	78009001	05-26-2000	158	4.43 ± 0.30 ^d
	78009002	05-28-2000	133	^e
	78009003	05-30-2000	188	3.80 ± 0.32 ^d
1415.2+4403	74075000	12-08-1996	76	1.55 ^f
1535.0+2336	60035000	07-26-1993	68	0.80 ± 0.26

^aGIS2+GIS3 count rate in units of 10^{-3} counts s^{-1} in the full ASCA band

^bGIS2+GIS3 archival net exposure time

^cAMSS (Ueda et al. 2002) count rate in the 0.7-7.0 keV band

^dThe source falls close to the border of the useful area of the GIS detectors; the value is a lower limit of the source count rate

^eThe source falls on the border of the useful area of the GIS detectors

^f 3σ upper limit in a 24 pixel (= 6') radius circle

TABLE 7
THE RADIO COUNTERPARTS TO THE BLANK FIELD SOURCES.

Source (1WGA J)	NVSS coord. Ra, Dec (J2000)	FIRST coord. Ra, Dec (J2000)	NVSS flux ^a (mJy)	FIRST flux ^a (mJy)
0221.1+1958	02 21 09.25, 19 58 07.2	not covered yet	7.9 ± 0.5	—
0432.4+1723	04 32 30.53, 17 23 41.0	not covered yet	3.2 ± 0.6	—
1226.9+3332	12 26 58.32, 33 32 44.3	12 26 58.186, 33 32 48.63	4.9 ± 0.6	3.61
1340.1+2743	13 40 10.93, 27 43 45.7	13 40 10.853, 27 43 46.96	4.6 ± 0.5	3.75

^a@ 1.4 GHz

TABLE 8
CLASSIFICATION OF THE BLANKS.

Source name (1WGA J)	Identification	z range	E ^a	O ^a	O-E ^b
1340.1+2743	BL Lac		-	-	-
0221.1+1958	Cluster	0.45	-	-	-
0432.4+1723	Cluster?	$\sim 0.5 - 1.0$	20.0	-	> 1.5
1103.5+2459	Cluster?	~ 1	18.2	-	> 3.3
1226.9+3332	Cluster	0.89	-	-	-
0951.4+3916	AGN?		19.1	-	> 2.4
1220.3+0641	AGN?		18.58	21.81	3.23
1233.3+6910	AGN?		-	-	-
1416.2+1136	AGN?		19.5	22.22	2.72
1412.3+4355	AGN	0.59	18.73	-	> 2.77
1415.2+4403	AGN	0.56	-	-	-
1535.0+2336	AGN?		19.6	21.8	2.2
1216.9+3743	X-ray binary?		-	-	-
1243.6+3204	X-ray binary?		-	-	-
1220.6+3347	Unknown		20.9	21.7	0.8
1420.0+0625	Unknown		-	-	-

^aPalomar data

^bwhen only the O or E magnitude is available we computed lower/upper limits on O-E assuming O=21.5 and E=19.5 as Palomar limits

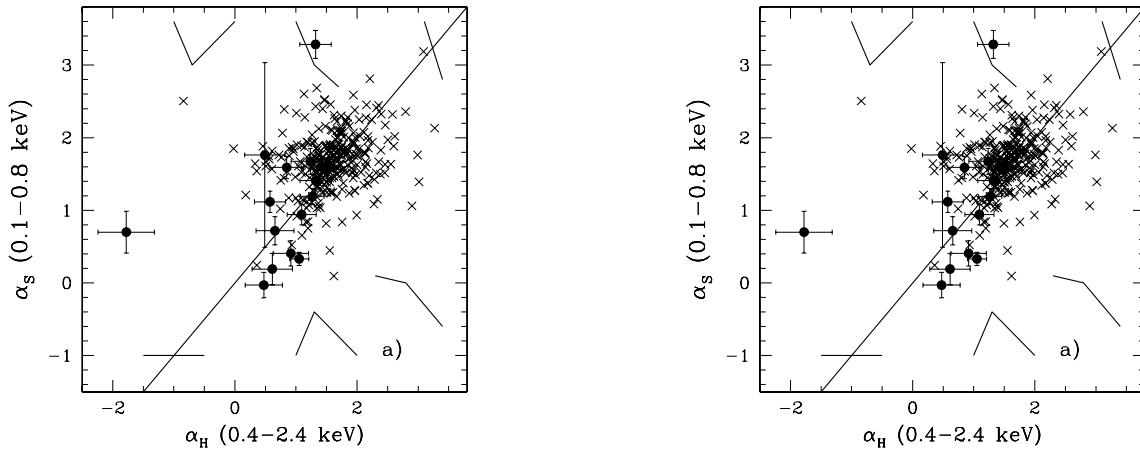


FIG. 1.— *ROSAT* PSPC effective spectral indices of blank field sources (filled circles) derived as in Fiore et al. (1998), compared to a reference sample of (a) radio-quiet quasars and to (b) radio-loud quasars from Fiore et al. (1998) (crosses). Three-point spectra illustrate the radically different spectral shapes in different parts of the diagrams.

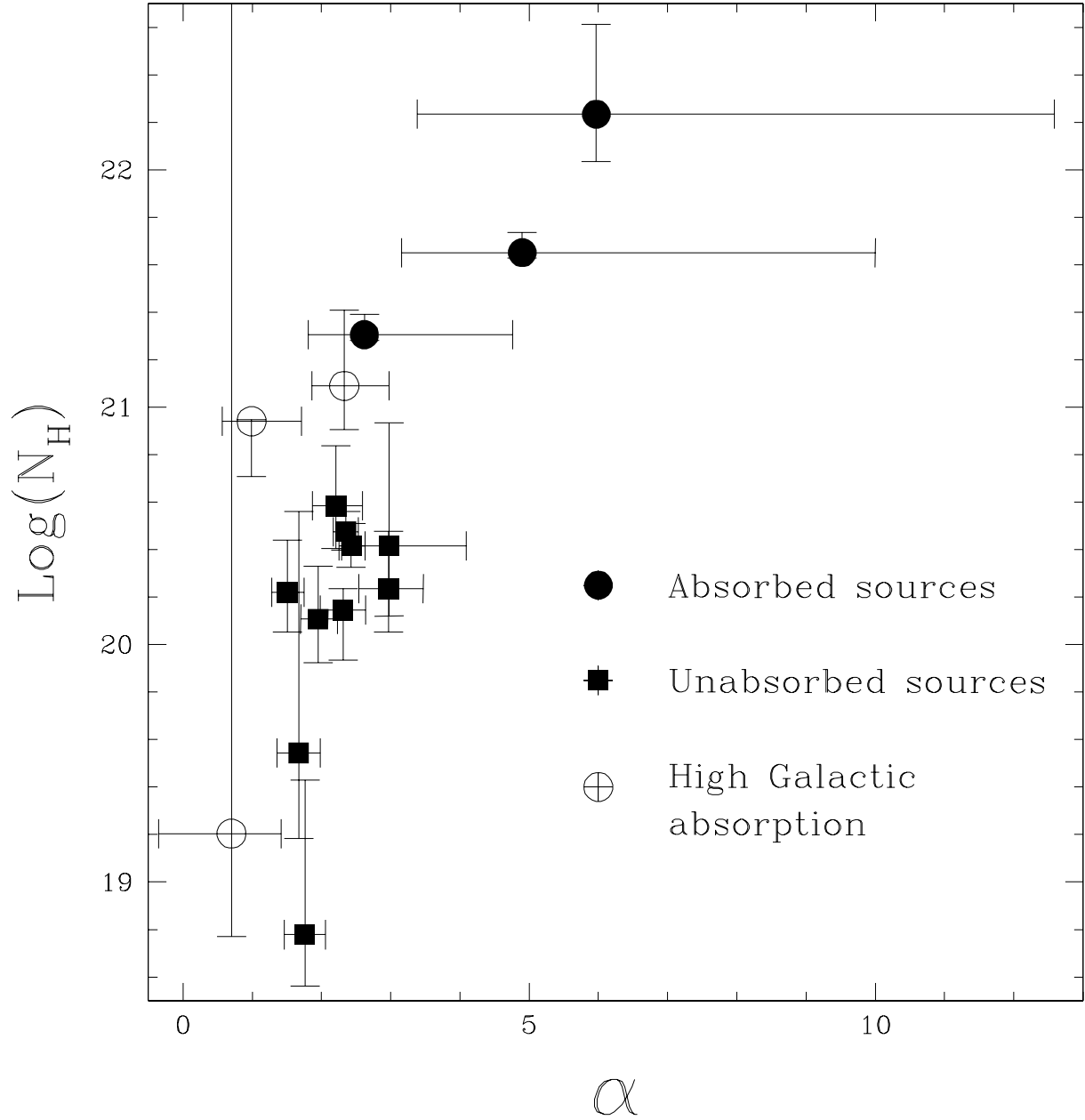


FIG. 2.— Absorption column versus energy spectral slope as derived from the fit with an absorbed power law model. Filled circles represent sources with indication of heavy absorption in excess of the Galactic value; open circles sources with high Galactic column density and squares the sources with absorption consistent with the Galactic value.

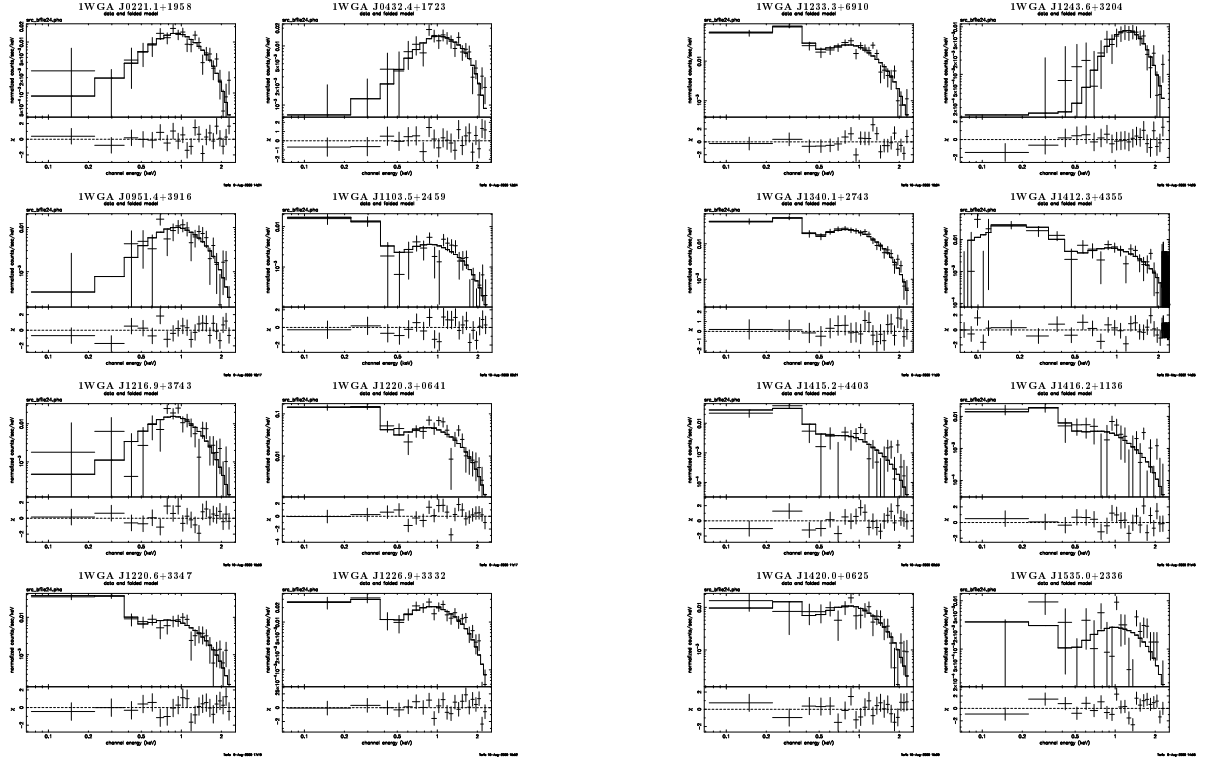


FIG. 3.— *ROSAT* PSPC energy spectra of the 16 blank field sources (upper panels); the solid lines represents the best fit with an absorbed power law model. The lower panels show the residuals.

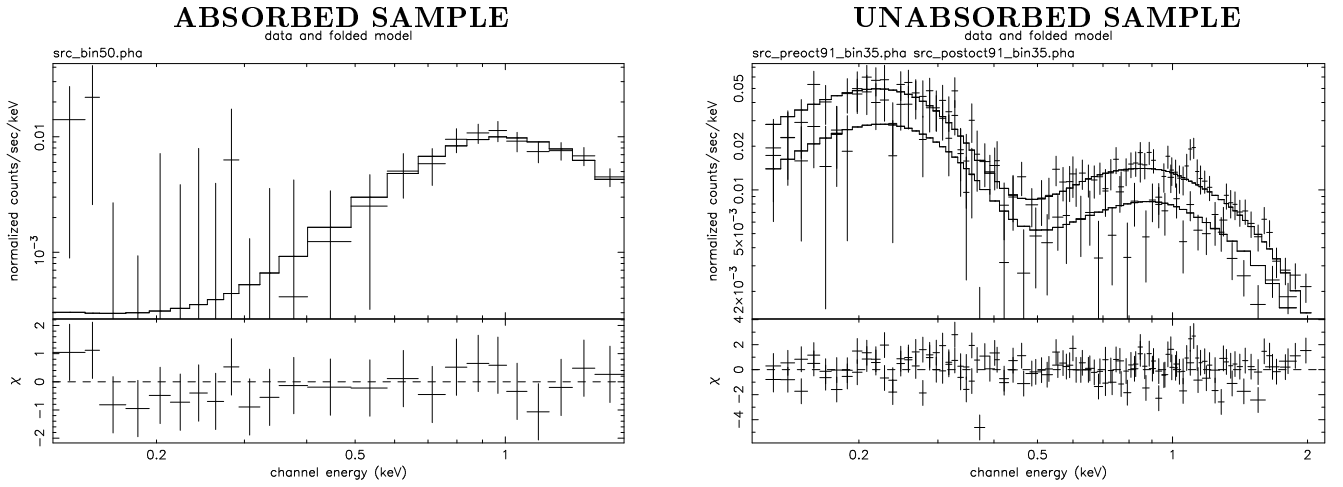


FIG. 4.— *ROSAT* PSPC combined energy spectra of the ‘absorbed’ (left) and ‘unabsorbed’ (right) samples and the residuals to the fit with an absorbed power law model with absorption fixed to the mean Galactic value of the sample (bottom panels) (see text for details).

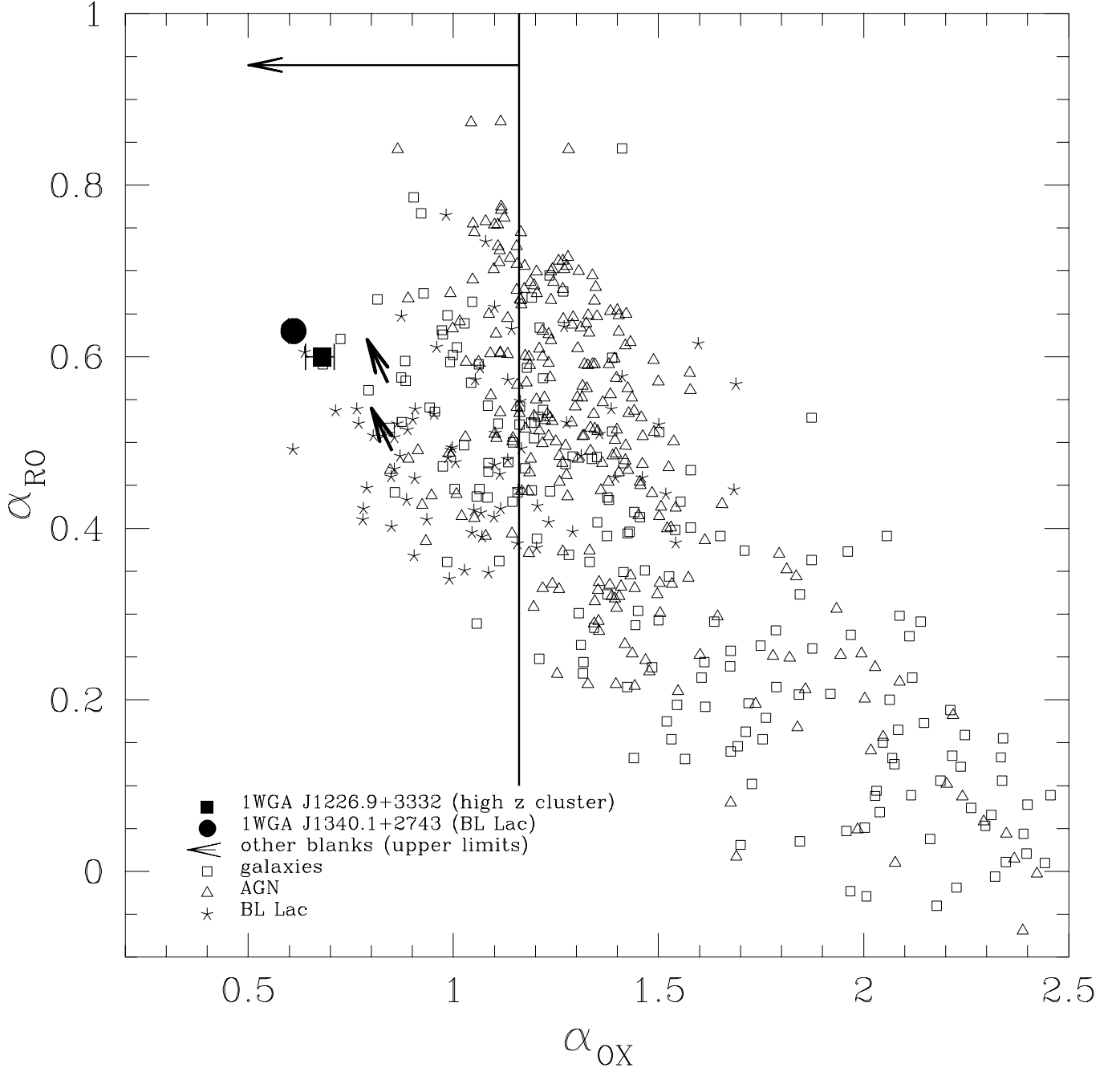


FIG. 5.— Broad band spectral indices for the 4 blank field sources with a radio counterpart compared to Caccianiga et al. (1999) sources (BL Lacs are represented by stars, emission line AGNs by open triangles and galaxies by open squares). The two filled symbols and the two nearby arrows represent the 4 blanks with a radio counterpart; in particular the square corresponds to the high z cluster 1WGA J1226.9+3332, the circle to the BL Lac object 1WGA J1340.1+2743 and the two arrows represent the limits for 1WGA J0432.4+1723 and 1WGA J0221.1+1958. The vertical line indicates the highest α_{OX} in our sample.

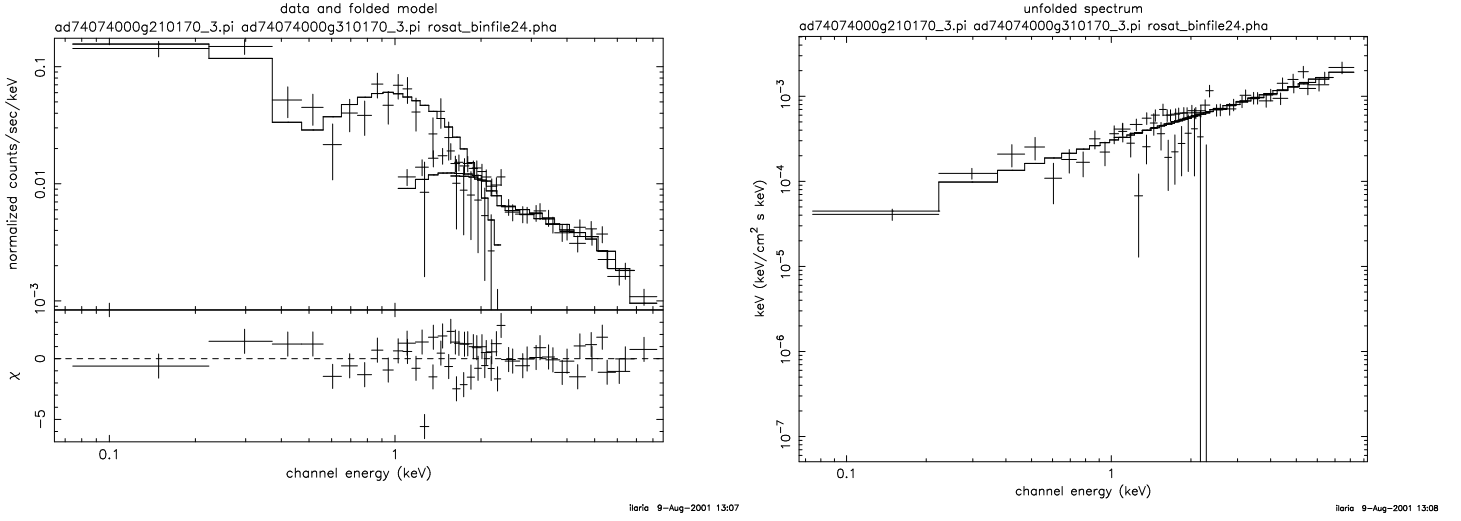


FIG. 6.— Left: *ROSAT* PSPC and *ASCA* GIS2 and GIS 3 spectra of 1WGA J1220.3+0641 and residuals to the fit with a powerlaw with absorption fixed to the Galactic value. Right: *ROSAT*–*ASCA* spectrum in the ν – $F\nu$ plane.

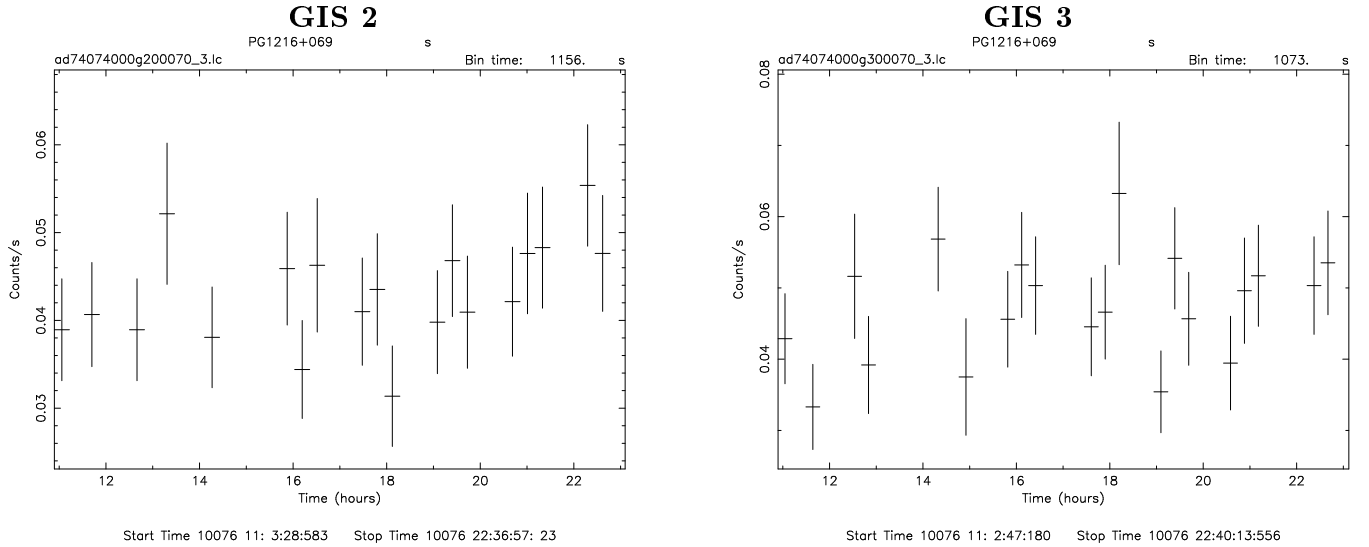


FIG. 7.— *ASCA* GIS2 (left) and GIS3 (right) archival lightcurves of 1WGA J1220.3+0641.

FIG. 8 —POSS II blue images of (left) NGC 4656 with the circle indicating 1WGA J1243.6+3204 position and (right) of NGC 4244 with the circle indicating the 1WGA J1216.9+3743 position (North is up and east is on the left; image sizes are $15' \times 15'$ for NGC 4656 and $20' \times 20'$ for NGC 4244).

This figure "icagnoni_f8.jpg" is available in "jpg" format from:

<http://arxiv.org/ps/astro-ph/0207085v1>